Proposal 97-106 (update) Studying the Internal Small-Distance Structure of Nuclei via the Triple Coincidence $(e, e'p + \mathrm{N})$ Measurement

J. Alster, D. Ashery, L. Frankfurt, A. Malki and *E. Piasetzky (spokesperson)*
Tel Aviv University, Israel

W. Bertozzi (spokesperson), S. Gilad, D. W. Higinbotham, M. Rvachev S. Sirca, R. Suleiman, Z. Zhou
Massachusetts Institute of Technology

B. Anderson, A. Baldwin, M. Manley, G. Petratos, D. Prout, *John Watson(spokesperson)* and W-Ming Zhang
KSU

John R.M. Annand, D. Hamilton, D. Ireland, G. Rosner, **University of Glasgow, Scotland**

D. Day, R. Lindgren, S. Koulechov, K. Wang, M. Zeier, **University of Virginia**

W. Boeglin, P. E. C. Markowitz, M. M. Sargsian, **Florida International University**

S. Heppelmann and M. Strikman, **PSU**

S. Danagoulian, **NC AT State University**

R. Carlini, R. Ent, K. Garrow, A. Lung, D. Mack, D. Meekins, W. F. Vulcan, B. Wojtsekhowski and *S. A. Wood (spokesperson)*
Thomas Jefferson National Accelerator Facility

K. Baker, C. Keppel., L. Tang and Y. Sato, **Hampton U.**

J. Templon , **University of Georgia**

K. Sh. Egiyan, G. V. Gavalian, H. G. Mkrtchyan, M. M. Sargsian and S. G. Stepanyan
Yerevan Physics Institute, Armenia

V. Nelyubin, V. Ryazanov, V. Tarakanov and M. Zhalov
Institute for Nuclear Physics, St.Petersburg, Russia

L. Weinstein , **Old Dominion University**

and the Hall A Collaboration

Contact Person: S. A. Wood, JLab

December 14, 2000

ABSTRACT

This is a new version of the proposal E97-106 that originally was submitted and approved in 1997 [1]. We propose to use the $(e, e'p + \mathrm{N})$ reaction on ^{12}C in hall A as a tool to measure short range nucleon-nucleon correlations (NN SRC). In the context of this proposal we refer to NN SRC has a pre-existing pair of nucleons which have back-to-back high momenta balancing each other. The two existing magnetic spectrometers will be used to measure the $(e, e'p)$ part of the reaction. The measurement requires a third spectrometer (BigBite) and an array of scintillation counters, to simultaneously measure neutrons and protons in coincidence with the outgoing high momentum electron and proton. We propose to use segmented scintillators as the only focal plan detectors for BigBite. This will simplify the Bigbite commissioning and allow high singles rates with sufficient resolution for this measurement.

We choose kinematical conditions that will allow us to determine the fraction of $(e, e'p)$ events which are associated with NN SRC. This will be done as a function of the momentum of the proton in the nucleus in the range 250-600 MeV/c. It will also allow us to compare between *pn* and *pp* correlated pairs in nuclei.

This proposal expands the existing limits to large Q^2, $x > 1$, and "exclusiveness" which were not covered by earlier data or other proposals to Jefferson Lab (JLab). We will discuss the importance of these kinematical constraints for the identification of NN short range correlations in nuclei and how they may overcome the obstacles from final state interactions, meson exchange currents and resonance production.

We would like to emphasize that this proposal is the only proposal to measure simultaneously both the $(e, e'p)$ as well as $(e, e'p + \mathrm{n})$ and $(e, e'p + \mathrm{p})$ reactions. We chose an optimized kinematics to minimize the competing processes and at this kinematics we will study the different contributions.

A letter of intent to perform a similar measurement on ^{3}He using the same experimental equipment as this proposal is being submitted.

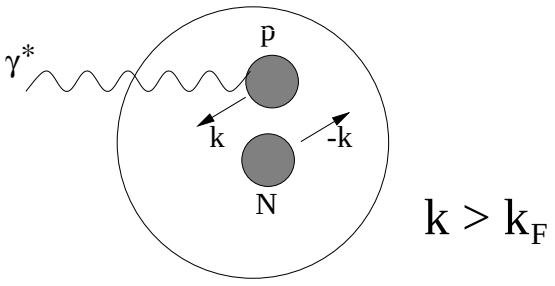

1 Introduction

1.1 Scientific background

Many basic nuclear properties can be described successfully within the single particle model. However, the simple picture breaks down when some detailed features are studied, especially in the extreme regions of the nuclear wave function. In recent years much attention has been paid to the role that two-nucleon correlations play in nuclei. Large high momentum tails in the nuclear spectral function were calculated with realistic potentials of two-and three-body interactions. A significant probability of NN correlations was predicted for light nuclei [2] for nuclear matter [3] and for an interpolation between these [4]. The field has been reviewed by Pandharipande et al. [5].

We will mention some experiments that address this issue. We will classify them by reaction, the final state, and by the kinematical parameters of the measurement.

There are inclusive (e, e') experiments [6, 7] at high momentum transfers and $x > 1$. They obtained the momentum distribution of the nucleons in the nucleus in terms of the y-scaling variable. Relatively large high-momentum tails are observed. Theoretical models try to explain this by invoking short range correlations [8]. Others [9] explained the results in terms of final state interactions (FSI).

There are (e, e') measurements in the "dip" region, between the quasi-elastic peak and the delta region, at $x \leq 1$ which show an anomalously large transverse cross section. This has been cited as evidence for NN correlations, although not necessarily short range. ([10, 11] and references in [11].)

$(e, e'p)$ experiments at small values of Q^2 and $x \leq 1$ [12, 13, 14, 15] observed a depletion of spectroscopic strength which may be explained by nuclear correlations which push the nucleons to higher momentum states and high missing energies and are thus not visible at low momenta and low excitation energies [11]. The depletion can be as large as 35% [5]. The Hall A Collaboration has used the ^{16}O$(e, e'p)$ reaction to study nucleon removal from the valence $1p$-shell [16, 17] as well as from the $1s_{1/2}$-state and higher residual excitations [18]. Measurements were done at a fixed four-momentum transfer, $Q^2 = 0.8(\mathrm{GeV}/c)^2$, and in quasielastic kinematics. The p-shell data and the low missing momentum s-shell data are well-described by relativistic DWIA calculations [20, 19, 18]. The spectroscopic factors extracted for the $1p_{1/2}$- ($1p_{3/2}$-) states were 0.73 (0.71) and 0.72 (0.67) for the Udias and Kelly calculations, respectively. A new theoretical approach can be found in [21]. The authors argue that the quenching of the single particle strength at large momentum transfer depends weakly on short range nucleon correlations.

Recently, two Hall A experiments E89-044 , [22], and E97-111 [23] studied the high momentum components of ^{3}He and ^{4}He using the $(e, e'p)$ reaction. In particular the ^{4}He measurement studied a possible signature for short range nucleon correlations in the two-body breakup channel. Other $(e, e'p)$ experiments [24, 25, 26], also at $x < 1$, show peaks at missing energies corresponding to the removal of two nucleons. There are also two- nucleon knockout reactions (e, ed) [27].

A new generation of "kinematically complete" experiments which measure the scattered nucleon in coincidence with the correlated one have been performed. This category includes $(e, e'pp)$ measurements from MAMI and NIKHEF [28, 29, 31, 30, 32, 33, 34, 35],and (γ, NN) from TAGX and LEGS [36, 37]. The new virtual photon measurements have the required energy resolution to identify the shells from which the proton pair was knocked out and to study the strength due to short range nucleon-nucleon correlations. Recent calculations [38, 39] also allow one to attribute that correlation to central (Jstrow type) and tensor components.

We would like to emphasize that all the NIKHEF and Mainz triple coincidence measurements were done at low Q^2. This proposal is very different than those. The high Q^2 is an essential element of it as will be pointed in the body of the proposal.

At the last DNP meeting the CLAS collaboration also presented preliminary results for the $^3\mathrm{He}(e, e'pp)n$ reaction [40, 41, 42]. Events corresponding to a single nucleon absorbing most of the virtual photon energy and two other nucleons emitted back to back with momenta above 250 MeV/c as well as events in which the photon is absorbed on a nucleon which is a member of a back to back high momentum nucleons pair, were identified. The simplest explanation of these events is to relate them to short range correlations in nuclei.

The next reaction we mention is the backward nucleon emission associated with scattering from nuclear targets. Experiments spanning a wide variety of projectiles and beam energies have been performed over the last 25 years [43, 44, 45, 46, 47, 48, 49, 50, 51, 52, 53]. These experiments have observed momentum spectra, angular distributions, and nucleon emission rates which are universal with respect to the various experimental conditions. This region of backward emission is defined so that it is not populated by interactions between the beam projectile and a single nucleon at rest. Therefore it requires the participation of two or more nucleons from the nuclear target. The universal emission pattern of nucleons with momenta large enough to exclude "boil off" from an excited nucleus has been interpreted as indication of initial-state short range correlations in nuclei [54, 52].

There are measurements of backward scattered protons from $(e, e'p)$ experiments at $x \leq 1$ [56] and deep inelastic (ν,μ p) [53] scattering where backward going protons were observed in coincidence with a forward going particle, electron and muon, respectively. Correlations were claimed between the transferred energy and the momenta of the backward going protons. In the last DNP meeting the CLAS collaboration presented preliminary results from the analysis of events with a forward scattered electron in coincidence with a backward emitted proton. These events indicate a sensitivity of the scattered electron spectra to the backward proton momentum and detection angle [57]. This is as expected from short range correlation dominance.

Last, but not least, we mention the experiment (E850) at BNL which studied the reaction $\mathrm{C}(p, 2 \text{ high } p_t \text{ particles} + n)$. The outgoing high p_t particles were detected in coincidence with a neutron with a momentum larger than 320 MeV/c. About half of the hard scattering events are in coincidence with at least one neutron emitted into the back

hemisphere. For the quasi elastic $(p, 2p)$ events, a correlation between the direction of the missing momentum and the emitted neutron momentum was found [58]. The simplest explanation of these two experimental observations relates them to the dominance of short range nucleon correlations. This experiment and the results will be discussed in section 1.3 and in Appendix I.

We propose to use the $(e, e'p+\mathrm{N})$ reaction on ^{12}C in hall A as a tool to measure short range nucleon-nucleon correlations (NN SRC). In the context of this proposal we refer to NN SRC as a pre-existing pair of nucleons which have back-to-back high momenta balancing each other. See Figure 1 for a graphical presentation. $\mathbf{k}$ and $\mathbf{k}'$ ($\mathbf{k} \simeq -\mathbf{k}'$) are the momenta of the two nucleons and k_F is the Fermi momentum surface. In an impulse approximation picture, the virtual photon is absorbed on one of the nucleons in the pair and the correlated partner nucleon is emitted in the opposite direction. We chose optimal kinematical conditions that will allow us to determine the fraction of $(e, e'p)$ events which are associated with pp and pn SRC. This will be done as a function of the missing momentum in the $(e, e'p)$ reaction in the range 250-600 MeV/c. In the simple picture that we use here, the missing momentum in the $(e, e'p)$ reaction is the momentum of the second nucleon which we are trying to detect.

1.2 Related Experiments and Proposals at JLab

The SRC between two nucleons in nuclei are a very elusive feature in nuclear physics. Their identification by the above mentioned experiments at low energies, is very difficult because they are small compared to the single particle components. It is also difficult to separate SRC from meson exchange currents (MEC), Isobar Contributions (IC) and FSI. Most of the experiments were done at $x < 1$ which sets the kinematics close to the delta production region and/or at low Q^2 where MEC and IC play a major role [26] and the FSI depend strongly on the proton energy.

Our proposed experiment expands the limits to large Q^2, $x > 1$ and the "exclusiveness" which were not covered by earlier data or other proposals to JLab. We will discuss, in section 2, the importance of these kinematical constraints for the identification of NN SRC in nuclei.

This proposal is a natural next step in the order of measurements and proposals that were done or approved at JLab, both from the scientific interest and from technical aspects. We hope to benefit from the knowledge and experience accumulated from double coincidence experiments in halls A and C and to add some unique knowledge to our understanding of the nucleus at short distances.

In the following, we will place the proposal among other proposals at JLab, according to the Q^2 and x scales.

- $x > 1$

  The overall amount of data at $x > 1$ is still scarce, largely due to small cross sections.

E89-008 [59] (Hall-C) is an inclusive (e, e') measurment that studies the $x > 1$ region.

E97-011 [60] (Hall-A) is an approved proposal to measure semi-inclusive $(e, e'p)$ on ^{3}He and ^4He targets.

Unpublished CLAS data - The overall amount of $x > 1$ data in this sample is probably very low.

This proposal is complementary to and augments the inclusive (e, e') and the semi-inclusive $(e, e'p)$ proposals and measurements. The semi-inclusive measurements contribute to our understanding of the microscopic origin of the high momentum tail by studying the spectral function as a function of p_m and E_m. The proposed triple coincidence experiment will allow us to study the decay function which is also a function of the momentum of the spectator nucleon. This is a much tighter measurement of the SRC contribution as we will discuss below. We propose to measure the contribution of 2N SRC to the high momentum tail as a function of that momentum. Data of this kind do no yet exist.

- Large Q^2

  Experiment NE18 was a breakthrough in the Q^2 range that was used in $(e, e'p)$ measurements. Earlier $(e, e'p)$ measurements were limited to Q^2 well below $1(\mathrm{GeV}/c)^2$ and NE18 opened up a new front at several $(\mathrm{GeV}/c)^2$. The proposed experiment together with CLAS provides a similar breakthrough for the more exclusive triple coincidence measurements. Data from NIKHEF and MAMI are limited to a small fraction of $1(\mathrm{GeV}/c)^2$. The new CLAS data are dominated by events at the $0.5 - 1(\mathrm{GeV}/c)^2$ range. Our measurement will be at $2(\mathrm{GeV}/c)^2$. These Q^2 are about two orders of magnitude higher than the non JLab triple coincidence data. The importance of large Q^2 to nail down the particular contribution from NN SRC will be discussed, in detail, further on.

- Exclusiveness

  This is the first proposal to do a triple coincidence experiment in hall A. There are no data or approved proposals to do such an exclusive measurement in hall A or hall C. The low cross sections we intend to measure (at the level of pb/sr^2 MeV) require the superior luminosity of one of these halls.

  Similar Exclusiveness can be seen only in the new data from CLAS studies of SRC using the reaction $(e, e'pp)$ in complementary kinematical regions, mainly $x < 1$ (see Refs.[61, 62, 63, 64]) and the $(p, 2p + n)$ BNL data.

A letter of intent to perform a similar measurement (triple coincidence, large Q^2, $x > 1$) on ^{3}He was submitted to this PAC. A new proposal to measure the electro disintegration of the deuteron under similar kinematical conditions to this measurement was also submitted to this PAC.

1.3 $A(p, 2p + n)$ Measurements at BNL

The reaction $A(p, 2p + n)$ was measured by us at BNL (E850) at beam momenta of 5.9 and 7.5$(\mathrm{GeV}/c)^2$. We established the quasi-elastic character of the reaction in a kinematically complete measurement. The neutron momentum was measured in triple coincidence with the two emerging high energy protons. We found a correlation between the momenta of the neutron and the struck target proton. The events were associated with the high momentum components of the nuclear wave function.

For a sample of events which is about an order of magnitude larger than the quasi-elastic events (events with two emerging high p_t particles) we also found that in sharp contrast to a well established universal pattern from inclusive measurements, about half of these events produce a backward neutron with momentum greater than 0.32 GeV/c instead of 10 percent for the inclusive measurements. We speculate that the enhanced backward neutron production in this semi-inclusive region could be an indication for a strong dependence in the cross section upon the total center of mass energy (s) and for the importance of short range nucleon correlations. If the cross section greatly favors low CM energy, a target nucleon in the nucleus moving in the direction of the incident beam has an enhanced probability to contribute to this process [65]. The hard scattering mechanism thus tends to select a nucleon from the nuclear wave function with an anomalously large and positive longitudinal momentum, typically at or above the Fermi momentum. If the high momentum component were associated with a short distance correlation between a proton and a neutron then we would expect most of the recoil momentum to be carried away by the correlated neutron partner. The correlated neutron should leave the nucleus after its partner has been scattered away, perhaps retaining the original large momentum and direction. More details are given in an Appendix I.

Based on our results from the (p,2p+n) reaction, we are encouraged to embark on a similar project with the electron probe. **Hopefully, with those measurements, together with the data we wish to collect at JLab, we will be able to approach a unified description of SRC in nuclei.**

1.4 Parasitic $^3\mathrm{He}(e, ep + n)$ Measurements in Hall A

Experiment E89-044 [22] ran in Hall A from December 1999 through March 2000 measuring $^3\mathrm{He}(e, e'p)$. In particular, part of E89-044 was aimed at the study of the high momentum components of ^{3}He using the $(e, e'p)$ reaction in perpendicular and parallel kinematics. During this experiment we made parasitic measurements of $^3\mathrm{He}(e, ep + n)$ using an array of scintillator bars to detect neutrons. The neutron bars were placed to measure the correlated neutron recoiling against the initial high momentum proton. ("Back to back") The third nucleon in ^{3}He (proton) is a spectator assumed to be at or close to rest in the nucleus. The ejected electrons and protons detected by E89-044 in $(e, e'p)$ were used to tag the additional neutron in $^3\mathrm{He}(e, ep + n)$. In the case of ^{3}He, this measurement is kinematically complete.

We measured two high missing momentum (p_m) points at perpendicular kinematics:

$p_{\rm m}$=300 MeV/c and $p_{\rm m}$=425 MeV/c. We also measured in parallel kinematics, one point with $p_{\rm m}$= 300 MeV/c. Altogether we collected about 25 M triggers which are about half of the triggers that the host experiment (E89-044) collected under these selected kinematical conditions. The data are being analyzed now. So far we do not identify a clear distinguishable peak in the measured neutron timing spectra. This has led to a preliminary upper limit of less than about 35% probability for a single high energy neutron emission per $(e, e'p)$ event with missing momentum of 300-450 MeV/c. See appendix II for more details. As will be discussed in this proposal, the kinematics for the parasitic measurement were not optimized for this research due to large contribution from FSI. Also, constraints due to the parasitic nature of the measurement prevented us from controlling the luminosity and shielding, resulting in a very high singles rate.

1.5 Proposed $A(e, e'p + \mathrm{N})$ Measurement at JLab

In many aspects, the electron-nucleus interaction is better understood than the nucleon-nucleus interaction. The electromagnetic interaction is weak compared to the hadronic one, and hence electrons probe the entire volume of the nucleus while hadrons tend to interact on the nuclear surface.

We propose to measure SRC at JLab in a quite similar way to that described in the previous section for the hadron-nucleus reaction. The proposed experiment will be significantly more precise and will have much better statistics than the experiment at BNL. Hall A has an excellent setup for measuring $(e, e'p)$ scattering. We plan to add a third arm consisting of a large acceptance magnetic spectrometer (to measure the protons) combined with a solid angle matched array of counters to measure neutrons in coincidence with the outgoing high momentum electron and proton. Just as for the (p,2p+n) reaction we will measure the full kinematics of the $(e, e'p)$ reaction, but with much higher accuracy enabled by the JLab facilities. As in $(e, e'p)$, we can extract the momentum of the struck proton. We will also measure the momentum and direction of an additional neutron or proton in coincidence with the outgoing e and p. **This will allow us to measure the fraction of $(e, e'p)$ events in which NN correlated nucleons are observed, as a function of the initial momentum of the proton in the nucleus.** It will also allow us to make a comparison between pn and pp correlated pairs in nuclei. We could not measure that ratio in the (p,2p+p) experiment because the targets were too thick and the low energy proton would lose a large amount of energy on its way out.

We refer to NN SRC has a pre-existing pair of nucleons which have back-to-back high momenta balancing each other. In this case: $\mathbf{p}_1 \simeq -\mathbf{p}_2$, $p_1, p_2 > k_F$, and $p_{cm} \simeq 0$, where in the laboratory system $\mathbf{p}_1$ and $\mathbf{p}_2$ are the momenta of the two nucleons and p_{cm} is their cm momenta, k_F is the Fermi momentum surface.

In an impulse approximation picture, the virtual photon is absorbed on one of the nucleons in the pair ($\mathbf{p}_m = -\mathbf{p}_1$, $\mathbf{p}_m$ is the missing momentum in the $(e, e'p)$ reaction) and the correlated partner nucleon is emitted with momentum $\mathbf{p}_2$ ($\mathbf{p}_2 = -\mathbf{p}_1 = \mathbf{p}_m$). See

Figure 1 for a graphical presentation.

We will choose kinematical setups that select scattering from protons above the Fermi sea ($p_m > k_F$). We will use an electron beam of 4 GeV (or above, if available), large momentum transfers in the region of $Q^2 = 2(\mathrm{GeV}/c)^2$ and missing energy in the region of $E_m = p_m^2/2m$. These conditions will minimize the contributions from FSI and MEC. Details of the kinematics and the experimental setup will be given in sections 2 and 3 of this proposal.

Why measure both neutrons and protons in the third arm? It is clear that one of the real exciting aspects of studying NN SRC is to understand it's isospin dependence. There are data on (γ, pp) and (γ, pn) [36, 37] and the ratio between the two cross sections. However, the measurements with real photons ($Q^2 = 0$) are sensitive to two-body currents which are not associated with short range correlations. (See section 2.3.2) Also, FSI may play a significant role in those data. Thus, the ratio between the SRC np and pp pair contributions is not well known and is one of the expected outcomes of the proposed measurement.

2 $^{12}C(e, e'p + \mathrm{N})$ Measurements at JLab

2.1 Kinematical Characteristics of NN SRC

One of the main consequences of the short range nature of a NN interaction is the strong correlation between *the momenta* of the correlated nucleons. Thus, for a pair at rest, when knocking out one of the nucleons, the second (spectator) nucleon will have a momentum (p_s) which is balanced with the initial momentum of the knocked out nucleon: ($\vec{p}_s \approx -\vec{p}_i$). Since SRC will exist predominantly in the high momentum tail of the nuclear wave function, such a spectator should have a large p_s , $p_s \geq k_F \approx 250\ MeV/c$. See Fig. 1 for illustration.

Fig. 2 shows the dominant process we wish to look for and defines the kinematical variables. We discuss the quasi-free break-up reaction of the pair at rest and we denote the pair, at rest in the nucleus, as d (quasi-deuteron). A similar description holds for a pp pair:

$$e + d \rightarrow e' + p + n \tag{1}$$

The kinematical conditions of the quasi-elastic reaction sets:

$$(q + p_d - p_f)^2 = m^2 \tag{2}$$

where $q = (q_0, \vec{q})$, $p_d = (m_d, \vec{0})$ and $p_f = (E_f, \vec{p}_f)$ are the four-momenta of the transferred momentum, the target pair and the detected final nucleon, respectively. ¿From the $(e, e'p)$ information we determine the missing momentum as $\vec{p}_m = \vec{q} - \vec{p}_f \approx -\vec{p}_i$ and the missing energy as $E_m = q_0 - (E_f - m)$. ¿From eq.(2) we obtain the following relation between missing momentum and energy:

$$E_m = \sqrt{m^2 + p_m^2} + m - m_d \approx \frac{p_m^2}{2m} \tag{3}$$

Thus in the breakup of a pair there is a strong correlation between the measured missing momentum p_m and the missing energy E_m.

In terms of the decay function which we discuss in detail in the next section , we concentrate on:

$$D(E_m = p_m^2/2m, p_m > k_F, \vec{p}_s \approx \vec{p_m}) \tag{4}$$

2.2 Description of the $(e, e'p + \mathrm{N})$ Reaction

The cross section for the reaction when a proton is knocked out of the nucleus and a spectator nucleon in the final state is detected in coincidence with the scattered electron and proton, can be represented within the plane wave impulse approximation , as follows:

$$\frac{d\sigma}{dE' d\Omega_e d^3(p_f/E_f) d^3(p_s/Es)} = K_d \sigma_{ep}(Q^2, \epsilon, E_m, p_m) \cdot D(E_m, \vec{p}_m, \vec{p}_s). \tag{5}$$

The decay function D represents the joint probability to find inside the nucleus, a nucleon with missing momentum $p_m(p_{m-})$ and missing energy $E_m(p_{m+})$ and where the residual nuclear state contains the spectator nucleon with momentum $\vec{p}_s(p_{s\pm}, \vec{p}_t)$. We use here light-cone variables in which any four-momentum k can be represented as $k \equiv k(k_+, k_-, k_t)$ where $k_\pm = k_0 \pm k_z$, where the z and t components are defined along the direction and perpendicular to the direction of the transferred momentum (virtual photon momentum) $\vec{q}$, respectively. Using the above definitions, we introduce the light-cone components of the missing momenta as $p_{m+} \equiv p_{f+} - q_+ = m - E_m + p_{mz}$ and $p_{m-} = p_{f-} - q_- = m - E_m - p_{mz}$. With the light cone momenta $p_{m\pm}, p_{s\pm}$ representation, we write:

$$\frac{d\sigma}{dE' d\Omega_e d^3(p_f/E_f) d^3(p_s/Es)} = K_d \sigma_{ep}(Q^2, \epsilon, p_{m+}, p_{m-}) \cdot D(p_{m+}, p_{m-}, \vec{p}_{mt}, p_{s-}, \vec{p}_{st}). \quad (6)$$

where K_d is a kinematic factor, $\epsilon = [1 + 2\frac{q^2}{Q^2} tan^2(\theta_e/2)]^{-1}$ and σ_{ep} describes the electron scattering on an off-shell proton.

The decay function is related to the spectral function of $(e, e'p)$ reaction in the following way:

$$\int D(E_m, \vec{p}_m, \vec{p}_s) d^3 p_s = S(E_m, \vec{p}_m) \quad (7)$$

or

$$\int D(p_{m+}, p_{m-}, \vec{p}_{mt}, p_{s-}, \vec{p}_{st}) d^2 p_{st} dp_{s-} = S(p_{m+}, p_{m-}, \vec{p}_{mt}) \quad (8)$$

The decay function defines the quantities which can be studied experimentally by a triple coincidence measurement.

2.3 Suppression of Competing Effects

The interpretation of existing low energy electron scattering data in terms of SRC has been plagued by contributions from two-body meson exchange and isobar currents and final state interactions whose importance depends on the transferred momentum and kinematical conditions. In this section we discuss how we choose the kinematics that minimize these effects. We discuss the relation of high momentum transfer to FSI effects and the conditions for which the FSI are well understood. In addition, the use of light-cone kinematical variables will be introduced which facilitates the conservation of variables that are important for the extraction of the initial momentum of the correlated nucleon pair. In this section we also discuss in detail the competing effects which can mask the SRC signal and how we intend to deal with them.

2.3.1 FSI, 'Almost Anti-parallel Geometry' and Light Cone Variables Analysis

Final state interactions (FSI) can mimic NN SRC event. This can happen, for example, if one of the outgoing protons scatters elastically from a neutron in the same nucleus at

an angle such that the recoil neutron enters the neutron counters. In this case the actual momentum ($\tilde{p}_m$) that the proton had before scattering from the electron is not what we are measuring $\vec{p}_m = \vec{p}_f - \vec{q}$. As a result one cannot be certain that the condition $p_m \geq k_F$, really probes the high momentum components in the nuclear ground state wave function. It will also smear the correlation between the neutron and the target proton momenta.

An important feature of the kinematics we are considering (large Q^2, $p_f \geq 1\text{GeV}/c$) is the applicability of the Eikonal approximation for the description of the rescattering. It means that small angle rescattering of GeV nucleons causes mainly transfer of momentum in the plane transverse to the direction of their high momentum (see [66, 67, 68]). This allows us to control, to some extent, the amount of FSI by selecting the angle between the target proton momentum and the incident virtual photon $\vec{q}$.

The best geometry for the suppression of FSI would be the parallel kinematics (see Fig. 3c). The large p_i and large q combine to a very large p_f which cannot be mimicked by FSI. Unfortunately, this geometry has some disadvantage. The large p_i and large q create a low x which entails contamination from resonance production.

In view of the above, we chose kinematics which we call "almost anti-parallel" (see Fig. 3e) in which we look at high momentum target protons (300-500 MeV/c) that are almost anti-parallel to the $\vec{q}$ direction ($x > 1$). If they are fully correlated with another spectator nucleon and the pair is at rest, and if we choose the direction of $\vec{q}$ properly, the spectator will be ejected at about 90 deg to the beam. This specific kinematical setup is a good compromise between the singles rates in the neutron counters (see section 3.2) and the suppression of FSI.

For light nuclei , $A \leq 16$, calculations of FSI diagrams within the generalized eikonal approximation (Ref.[69]) shows that in addition to $x > 1$, the condition:

$$|p_{mz} + \frac{q_0}{q} E_m| \geq k_F \tag{9}$$

will confine the rescattering with another nucleon to within short range. As a result the FSI will take place mainly with the nearby partner nucleon in the correlation. Thus, it will not spoil the SRC characteristics of the process.

In addition, we will use light cone variables for the analysis of the data because they are less sensitive to FSI effects, as follows. With the light cone momenta $p_{m\pm}, p_{s\pm}$ the cross section of the reaction was given in equation eq.(6). In our case the specific decay function we wish to measure is:

$$D(p_{m-} \approx 2m - p_{s-}, p_{m+} \approx ({m^2} + {p_{ts}}^2)/(2m - p_{s-}), \vec{p}_{tm} \approx \vec{-}p_{ts}) \tag{10}$$

The advantage of describing high energy transfer reactions ($q \geq 1$ GeV/c) with light cone variables lies in the fact that, while E_m and $\vec{p}_m$ change due to FSI, the combination of p_m and E_m in the form of the p_{m-} (or $\alpha = p_{m-}/m$) survives the FSI[70, 69]. The accuracy of the conservation of p_{m-} is given by [69]:

$$\tilde{p}_{m-} - p_{m-} \approx \frac{Q^2}{2q^2} E_m, \tag{11}$$

where the $\tilde{p}_{m-}$ is the corresponding momentum of the target nucleon before the interaction. It follows from this equation that the conservation of p_{m-} improves with increasing energy.

Thus one might expect that the description of the SRC in terms of (E_m, p_m) could be complicated by FSI, while it will be preserved in terms of the p_{m+}, p_{m-} (or α) representation.

Just to estimate the effect due to FSI we used a simulation with an event generator of electron-nucleus reactions (see Sargasian [71]). The essential assumptions behind this event generator are:

- The cross section is calculated on the basis of the light cone impulse approximation [54] using an off-shell model for σ_{eN} [72, 73].
- The spectral function is obtained by assuming a simple Fermi gas model for nucleons with momenta below $k_F = 220$ MeV/c and two nucleon correlation dominance above the Fermi sphere. For the latter we used a two-nucleon SRC model based on references [54] and [4].
- We assumed that the FSI can be described in a standard Glauber approximation [74].

Using the event generator we produced events and selected only those that fulfill the kinematical constraints imposed by the experimental set up or by software cuts we will apply to select the SRC events (according to the kinematics). The list of imposed constraints is given in the table below:

scattered electron: $p = 3.16 - 3.28$ GeV/c, $\theta = 23 \pm 1.25°$, $\phi = \pm 3.5°$

scattered proton: $p = 1.05 - 1.57$ GeV/c, $\theta = 40 \pm 3.5°$, $\phi = 180 \pm 2.5°$

neutron (third arm): $\theta = 90 \pm 10°$,$\phi = 180 \pm 10°$

The simulation was done for an incident electron beam of 4 GeV/c. Originally we defined the simulation according to the momentum and angular acceptances of the hall C spectrometers (SOS and HMS). The hall A HRS_e and HRS_h spectrometers have smaller acceptances than in the simulation results presented here.

The events that passed the kinematical cuts were categorized in 3 groups:

- type A. QE events: the virtual photon interacts exclusively with a single high momentum nucleon and kicks it out of the nucleus. The correlated spectator neutron emerges in the opposite direction (in their cm system). The process is shown schematically in Fig. 4.
- type B1. Rescattered events: The virtual photon interacts with a single nucleon. This nucleon is rescattered off another neutron in the nucleus. The result of this rescattering is a neutron with momentum (p_R) in the third arm and a wrong reconstructed initial momentum of the proton $(\tilde{p}_m \neq p_m)$. See Fig 4.

- type B2. Rescattered events: Same as type A events but at least one of the protons gets rescattered and causes a wrong reconstructed initial momentum of the proton ($\tilde{p}_m \neq p_m$). The neutron in the third arm in this case is a real correlated neutron. See Fig 4.

- type C. Other inelastic process as well as short range FSI take place with the nearby partner nucleon of the correlation. These events are simulated also by the event generator but will be ignored for this discussion (they are a small fraction of the total events in our kinematically constrained sample).

Simulated spectra of the missing momenta and the neutron momenta were obtained with the event generator and the applied cuts. The events of type A are 82% of the total events ($p_m = 300 - 600 MeV/c$). The events of type B2 (FSI) are about 9% of the total events The events of type B1 are only 5×10^{-4} of the total events. If we also require the neutron of events B1 to be above 300 MeV/c we do not find even one such event which puts the upper limit on the contamination of type B1 events at about 5×10^{-5}.

2.3.2 MEC, Isobar Contributions, Large Q^2 and $x > 1$

It is difficult to isolate the effects due to nucleons at close proximity from those caused by two-body effects such as meson exchange currents, isobaric currents and other long range correlations. Also, final state interactions (as discussed in the previous section) can mimic large nucleon momenta and the signature for SRC. High Q^2 is the best way to select the SRC. The sensitivity to short ranges increases as the virtuality of the photon increases. The MEC diagrams have additional $1/Q^2$ dependence compared to the diagrams where the electron scatters from a nucleon. Competing two-body effects diminish as $1/Q^2$ and are also reduced for $x > 1$ (see [75, 76]). The FSI become less important at high Q^2 and become easier to deal with by using light cone variables. For quasi-elastic scattering the knocked out proton moves in the forward direction with high energy and the eikonal approximation can be used in the calculations. Also, the high energy of that proton makes it easy to distinguish it from the spectator correlated hadron.

Within the kinematics of quasi-free scattering, we represent in Fig.5 the relations between the missing momenta and the Bjorken variable $x \equiv \frac{Q^2}{2mq_0}$ for different values of Q^2. Here $q_0 \equiv E_e - E'_e$ and $Q^2 = 4E_eE'_esin^2(\theta_e/2)$ are the transferred energy and squared four-momentum to the nucleus, E_e, E'_e are the energy of the initial and scattered electrons and θ_e is the angle of the scattered electrons with respect to direction of the initial electron.

One can see in Fig.5 that both the $x < 1$ (parallel geometry) and $x > 1$ (anti-parallel geometry) regions provide large values for the missing momentum. Thus experiments which aim to study the high missing momentum should explore one of these two regions.

Fig.5 also shows that in order to achieve some large missing momentum, a larger Q^2 is needed for the $x > 1$ region. This was the reason why low energy experiments mainly explored the $x < 1$ region. However, all experiments in the region of $x < 1$

have the disadvantage of being near the inelastic threshold for pion production. This situation becomes more acute with increasing energy transfer. For example, for nuclei with $A \geq 12 - 16$ the broad Fermi distribution causes the inelastic contribution to be as high as 40% of the (e, e') cross section at $Q^2 = 2$ $(\mathrm{GeV}/c)^2$, even at $x \approx 1$[8, 59]. The exclusiveness of the triple coincidence reaction of the proposed experiment reduces that contribution drastically.

To simulate the contribution due to Δ production Sargsian [71] used Bodek et al. [77] to parameterize the $\gamma^*\ N \rightarrow \Delta$ vertex. Then a $\Delta\ N \rightarrow \Delta\ N$ and $\Delta\ N \rightarrow N\ N$ rescattering is done using phenomenological amplitudes.

No "Δ production" event passed the kinematical cuts we impose to select the QE events. The reason is shown in Fig 6. The "Δ production" events have an ω larger than accepted by the QE setup. The rescattered nucleon also emerges mainly at forward angles out of the acceptance of the third arm. The combined limitation left us without any event originating from Δ production.

All this leads to an exclusive measurement of three particles in coincidence in a region of high energy, high Q^2 and $x > 1$. We choose to pay the price of the small cross section at $x > 1$ in order to decrease contributions from resonance effects.

In a triple coincidences measurement, in general, the assignment of the initial momenta of the two detected nucleons is not unique, depending on whether the virtual photon is being absorbed by one or the other nucleons. There are two amplitudes which add up coherently. The ambiguity is a problem in low Q^2 measurements. In the specific case of this proposed large Q^2 measurement the high momentum transferred identify clearly the "forward" nucleon that absorbed the photon from the correlated "backward" emitted partner. In principle one has to coherently add two amplitudes, but in this case one of the amplitude is too minute to be considered. This is another important advantage to doing the measurement at high Q^2.

Since the high Q^2 is such an essential element of this proposal we would like to summarize the advantage of the high Q^2 measurement:

- Competing processes such as MEC are reduced as $1/Q^2$.
- It allows for a better understanding of FSI which can be treated in a Glauber scattering formalism, and in light-cone kinematics in which the relevant coordinates are conserved.
- It reduces significantly the ambiguity which exists in low Q^2 measurements with respect to the the identification of the struck and recoil nucleons.
- It allows us to perform the experiment in "anti-parallel" kinematics ($x_B > 1$, in this case it is about 1.5), which is favorable in reducing MEC and IC and in enhancing SRC.

2.3.3 The Selected Kinematics for the Measurement

The experiment we propose is a triple coincidence measurement of a fairly low cross section (pb/sr^{2}MeV) corresponding to a very elusive feature in nuclear physics. The neutron array, due to the heavy shielding, is not easy to move. This means that we have to carefully choose a single, optimized kinematical setup for the measurement. As we discussed in the previous sections, we choose a large incident energy, large Q^2, large target proton momentum, large x, and "almost anti parallel" geometry.

The proposed kinematical setup is shown in Fig 7 together with the range of kinematical variables to which we will be sensitive. We propose to do the measurement at $Q^2 = 2$ (GeV/c)^2 with enough statistics for exploring the momentum tail up to 600 MeV/c.

3 Experimental Considerations

3.1 Experimental Set Up

Hall A has two spectrometers (HRS_h and HRS_e)which are routinely used for $(e, e'p)$ coincidence measurements [78, 17, 18, 22, 23]. All necessary equipment, including electronics and data acquisition are available for this "standard" setup. The off-line data analysis for the $(e, e'p)$ part of the measurement is working routinely. A few experiments have already published results from hall A $(e, e'p)$ measurements.

We plan to add the BigBite spectrometer with modifications, to measure neutrons and protons in coincidence with the outgoing high momentum electron and proton.

BigBite is a non-focusing large momentum and angular acceptance magnetic spectrometer that was originally designed and built for use at the internal target facility of the AmPS ring at NIKHEF [79, 80]. The spectrometer consists of one dipole (maximum magnetic field: 1.2 Tesla) and a detection system that includes two sets of wire chambers, a plastic scintillator, and an aerogel Cherenkov detector. At the maximum field settings electrons are accepted with a momentum between 250 and 900 MeV/c and moderate momentum resolution of Δp/p=0.8 %. Figure 8 is an artist's view of the BigBite spectrometer showing the magnet and the detector system.

The BigBite spectrometer was procured from NIKHEF by JLab and UVA and is currently being tested as a candidate third arm in Hall A [81]. The addition of a large solid angle and momentum acceptance spectrometer to the two existing high resolution spectrometers will enable three arm measurements or experiments which need high resolution in one arm and a large solid angle in the other.

The main problem in adapting BigBite is the fact that it was designed for the low-luminosity NIKHEF environment. In Hall A the luminosity can be factors 10^4 - 10^6 higher than at NIKHEF and the counting rates in the focal place detection system will be correspondingly higher.

The detector package has been rebuilt at JLab by JLab and the UVA group and has been tested using cosmic rays. A group from Glasgow lead by Prof. Rosner is already committed to upgrading the BigBite by providing new trigger detectors, replacing the present unsegmented scintillator layer. They plan to build two layers of segmented plastic scintillators. One layer (ΔE) will consist of thin counters (3 mm) and the E counters will be 3 cm thick counters. Each plane will be segmented into 16 elements, each segment to be read out via twisted-strip light guides by two fast 50 mm photomultipliers (PM). The geometry of the Glasgow two-plane system is sketched in figure 9. This system as proposed will provide a position-independent mean time with resolution of 0.5 ns FWHM or better, position information in the non-dispersive direction (4 cm FWHM) and ΔE/E information. In the first stage the system will use the original drift chambers. It is not yet clear what the luminosity limit will be.

To perform the triple coincidence measurement of short range correlations using the $(e, ep + p)$ reaction as outlined above, we propose to build a third plane of segmented

plastic scintillators located near the effective field boundary (EFB), as shown in figure 10. The time of flight (TOF) between this plane and the Glasgow counters, together with the hit pattern will determine the momentum of the particles with a resolution sufficient for the proposed measurement (see details below). This can be achieved even without using the drift chambers. In that option the single rate limit will be about 10 MHz (less than 1MHz per counter). We also propose to redesign the geometry of the Glasgow detectors to allow larger distance between the scintillator planes for this mode of operation. Calculations of the resolution for the current position of the original single scintillator and double this distance, are shown below.

BigBite will measure the $(e, ep + p)$ reaction as outlined above. For the proposed experiment we also plan to install an array of plastic scintillators at about 6 m from the target with a solid angle matched to the spectrometer, to detect the neutrons (see Fig 11A) in the reaction $(e, ep + n)$. We will use available plastic scintillators from TAU, KSU, and UVa. We plan to stack the detectors in a horizontal position with the center of the array at beam height. We plan to use four walls with 10 scintillators (160x10x10 cm^3) in each wall. The first wall will serve as a veto of charged particles. The total width of active 30cm in the detection direction will allow a neutron detection efficiency of about 35%.

The 35% efficiency mentioned is a rough estimate for the purpose of calculating the rates and beam-time request. The efficiency as a function of momentum is well known. These detectors have been used before, and hence their efficiencies have been studied, including a simulation for the BNL experiment according to the method described in ref. [82].

See figure 11B for the proposed experimental setup. Together with the neutron counter array, BigBite will serve as a high rate neutron/proton detector. The magnetic field will allow momentum analysis of the protons and will sweep away the charged particle from the neutron counters, thus reducing the singles rate on the neutron counters. We will also be able to install a relatively thick lead shield in front of the neutron counters since we do not plan to use them to detect the protons, as originally designed.

The trigger for this experiment will be an electron-proton coincidence in the two HRS spectrometers. We will read out the BigBite and neutron bars whenever we get that trigger.

3.1.1 Expected Momentum Resolution (BigBite)

To estimate the momentum resolution we used a GEANT simulation of BigBite (courtesy of Vladimir Nelyubin). We assume that the segmented plastic scintillators are 12.9cm thick, that the two scintillator planes are parallel and are 96.38 cm apart or twice this distance. The first distance corresponds to mounting one plane at the effective field boundary and the other plane at the position of the original unsegmented scintillator. The double distance assumes that the $\Delta E/E$ counters will accommodate such a move. We assume that the EFB counters will be 5 mm thick and that the resolution in the TOF

measurement between the two planes will be 1 ns. Momentum definition will be done by both track reconstruction (using the segmented scintillators) and timing. We have performed GEANT simulations with both methods. The GEANT simulation includes the effect of the energy loss in the C target. We did not simulate the effects of the scattering chamber windows in this preliminary GEANT simulation, but they should not be big compared to the 1mm C target. The results are summarized in table 3.1 and are also shown in figures 12.

Table 3.1

proton momentum	300 MeV/c	400 MeV/c	500 MeV/c	600 MeV/c
distance between scint. planes (cm)	momentum resolution MeV/c (%)	MeV/c (%)	MeV/c (%)	MeV/c (%)
96.38	±8 (2.7)	±23.5 (5.9)	±44. (8.8)	±70.(11.7)
192.76	±5. (1.7)	±12. (3.0)	±22.5 (4.5)	±34. (5.7)

As can be deduced from the table, we can measure the proton momentum with resolution better than ±25 MeV/c up to 500 MeV/c. This is to be compared with the expected n momentum resolution (better than 12.5 MeV/c) and the size of the missing momentum bins of the $(e, e'p)$ part of the measurement which will depend on the obtained statistics. The latter is expected to be 50 MeV/c .

3.1.2 Particle Identification (BigBite)

For the worst case, 600 MeV/c, the time difference between pions and protons will be about 2 ns for 96.4 cm between the planes and about 4 ns for twice that distance. The light produced in the scintillators for 600 MeV/c pions is about half that for 600 MeV/c protons. So, within the range of interest for this proposal, we should be able to identify pions from protons in BigBite.

3.2 Parasitic Background Measurements in Halls C and A

Measurements in hall C were performed by Sudhir Malik (TAU) with the help from Steve Wood (JLab)and Eli Piasetzky (TAU). The measurements were done in November 1997 in a parasitic mode during exp. 93-021 .

A schematic view of the experimental set up in hall C is shown in Fig 13. The counters were $12.5 \times 10 \times 30 cm^3$ plastic scintillators with 2 inch PM's on both sides. The paddle

was a $12.5 \times 30 \times 1 cm^3$ plastic scintillators with one PM. The counters were shielded on top, front and back by 2 inches of Pb and below by 3 meter of concrete. There was no shielding on the sides.

The measured singles rates in counter 1 (left PM), in units of nucleon luminosity, are presented in table 3.2.

Table 3.2

run	energy(GeV)	SOS angle(deg)	current (μA)	target	rat./lum.[10^{-36}cm^2]
1	1.8	20	5.5	C 1mm	688
2	1.8	20	5.5	C 1mm	655
3	1.8	20	5.5	C 1mm	619
4	1.8	20	6.1	H 4cm	291
5	1.8	20	6.1	D 4cm	287
6	2.68	36.5	7.4	D 12cm	328
7	2.68	36.5	74	D 4cm	218
8	3.547	45.36	7	H 4cm	385
9	3.547	45.36	93.5	H 4cm	268
10	3.547	21.87	43.5	D 4cm	248

It seems that, within the relevant range, we can assume about a constant singles background of $(300) \times 10^{-36} cm^2$ for H/D. The measured carbon rates are about a factor of 2 higher.

If we assume that the rates are target-dominated and if we scale the results by the solid angles we get for a counter at 3 meter distance from the H/D target:

rate/lum = $(300 \times 10^{-36}\text{cm}^2) \times (5.3/3)^2 = 1000 \times 10^{-36}\text{cm}^2$

Thus, in the original proposal submitted in 1997 we assumed that the background rates are $2 \times (3 \times 10^{-33}) \times (nucleon\ luminosity)$ in a standard $12.5 \times 10 \times 100 cm^3$ counter at 3m from a C target.

A second parasitic measurement was done in Hall A during the beginning of 2000 together with experiment E89-044 [22]. We set 28 $12.5 \times 10 \times 160\text{cm}^3$ counters at 120° and about 5m from a 10cm 0.06 gr/cm^2 ^{3}He target with similar shielding to that used in the Hall C measurement. We measured singles rates of about 0.725MHz per scintillator counter of the front wall (with detection thresholds of 10 MeV proton). This is consistent with the rough estimate we establish based on the previous hall C measurements:

$(6 \times 10^{-33}) \times$ (nucleon luminosity) $\times (160/100) \times (3/5)^2$
$= (6 \times 10^{-33}) \times (2.25 \times 10^{38}) \times (160/100) \times (3/5)^2 = 0.8$MHz

We therefore, based on our measurements, expect the singles rates on a neutron counter in the proposed setup to be:

168 kHz for 100 μA on a 1 mm C target.

From our experience in analysis of the data only abot 70% of the events passed the software cuts required to define a "neutron" in the scintillator array. The effective singles rate on a neutron counter in the proposed setup is therefore:

- 120 kHz for 100 μA on a 1 mm C target.

3.3 Rates

For the purpose of estimating the counting rate we assumed that, at the high momenta we are focusing on (p_m=300-600 MeV/c), all counts are due completely to 2N SRC. We also assumed that under this condition the measured cross section can be expressed as

$$\frac{d\sigma}{dE_e d\Omega_e d\Omega_p} = K_0 \times a_2 \times Z \times \frac{d\sigma}{dE_e d\Omega_e d\Omega_p}_d \tag{12}$$

where $\frac{d\sigma}{dE_e d\Omega_e d\Omega_p}_d$ is the calculated deuteron differential cross section [70, 83]. a_2 is a scaling ratio obtained from high Q^2 inclusive (e,e') scattering at $x > 1$ Ref.[8]:

$$\begin{aligned} a_2(^3He) = 1.7 \pm 0.3, \quad a_2(^4He) = 3.3 \pm 0.5 \quad a_2(^{12}C) = 5.0 \pm 0.5 \\ a_2(^{27}Al) = 5.3 \pm 0.6 \quad a_2(^{56}Fe) = 5.2 \pm 0.9 \qquad a_2.(^{197}Au) = 4.8 \pm 0.7 \end{aligned} \tag{13}$$

and K_0 is a kinematical factor related to the np-pair cm momentum in the nucleus. We used a conservative estimate of 0.2 for it [83]. In Table 3.3 the estimated differential cross sections for $E_e = 4$ GeV at $Q^2 = 2$ are presented.

Another way to estimate the cross section for the proposed measurement is to rescale the lower energy measured cross section for exclusive deuteron disintegration from Ref.[84]. This experiment was done at approximately the same missing momenta as in the present proposal but with $Q^2 = 0.0377$ (GeV/c)^2. To rescale this cross section to the region of $Q^2 \approx 2$GeV^2, we assume that, because of the cancelation between FSI and MEC contributions in the kinematics of Ref.[84], the PWIA calculation may describe fairly well the data [84]. Thus we use the factorized form of the PWIA approximation $\sim \sigma_{eN} \psi_D^2(p_m)$ and rescale the σ_{eN} to the kinematics of this proposal. For this we use the different off-shell models for σ_{eN} (see e.g. [85]). Within 20 % the results are the same for all the models used [83]. Taking the measured value $d\sigma/dEd\Omega_e d\Omega_p \approx 30 pb/MeV/sr^2$ at $p_m \approx 500\ MeV/c$ and rescaling for σ_{eN} one obtains $\approx 0.06 pb/MeV/sr^2$. Then taking into account the $z \cdot a_2 \approx 30$ factor one obtains $d\sigma/dEd\Omega_e d\Omega_p|_{Q^2=2\ (\mathrm{GeV}/c)^2} \approx 1.8$pb/MeV/sr^2. This is the same value as shown in Table 3.2 which was obtained by the estimate based on the (e,e').

We have also contacted Ryckebusch for estimates of the expected $(e, e'pp)$ and $(e, e'pn)$ cross sections. Jan will try to make some "educated guesses" for the cross sections of the proposal kinematics based on the results of his published calculations [38, 39]. We should point out, though, that it is not at all clear that calculations such as those of are reliable at $Q^2 \simeq 2$.

The ratio between the SRC np and pp pair contributions is not known and is one of the expected outcomes of the proposed measurement. For counting rate estimates we assume that $(np)/(pp)$ is between 2 (based on statistical isospin weight) and 4.

For the experimental acceptances and the proposed kinematical ranges we used the following values:

- $\Delta E_e = |E_e(p_m = 350 MeV/c) - E_e(p_m = 300 MeV/c)| = 20 MeV$
- $\Delta\Omega_e = \Delta\Omega_{HRS_e} = 6 msr$
- $\Delta\Omega_p = \Delta\Omega_{HRS_h} = 6 msr$
- n detection efficiency = 0.35
- n attenuation in the lead shield =0.5
- n attenuation in the first layer of counters (used as veto only) =0.9

The luminosity will be limited by the background singles rates on the plastic scintillators of the the third arm.

In Tables 3.3, we present signal counting rates based on the above assumptions and a luminosity corresponding to 100 μA beam, a 1 mm thick C target, and the differential cross sections of columns 2. The total number of events per hour of beam are shown in columns 3 for np pairs (n detected by the third arm) and in columns 4 for pp pairs(p detected by the third arm). The measurements will be perform with three central momentum of the HRS_e and HRS_h, each covering a p_m range of about 100 MeV/c. The time devoted for each setup is shown in the first column of Table 3.4 with the expected total number of measured (np) and (pp) pairs (column 3 and 4 of Table 3.4).

Table 3.3

$p_m[MeV/c]$	$\frac{d\sigma}{dE_e d\Omega_e d\Omega p}$ $(pb/sr^2 MeV)$	counts/hr (np pairs)	counts/hr (pp pairs)
250± 25	(*)17.2	(*)43	(*)170-340
300± 25	7.2	18	70-140
350± 25	3.2	8	30-60
400± 25	1.8	4.5	20-40
600± 50	0.3	1.5	6-12

Table 3.4

$p_m[MeV/c]$	time [hr]	total counts (np pairs)	total counts (pp pairs)
250± 25	100	(*)4300	(*)17,000-34,000
300± 25		1800	7,000-14,000
350± 25	150	1200	4,500-9,000
400± 25		675	3,000-6,000
600± 50	200	300	1,200-2,400

(*) At this low momentum the dominance of SRC 2N contribution is very questionable. We add this point to measure the onset of the phenomena as the momentum p_m increases.

A calibration of the neutron detectors can be done with the reaction $d(e, e'pn)$ using a single setting of the spectrometers. For this measurement we assume the same nucleon luminosity as for the carbon. The cross section on the deuteron is about a factor of 6 smaller than the carbon cross section but the 6 times higher nuclear luminosity makes the count rates about equal. Using the low p_m setup, in 10hr we expect a peak of 400 well defined neutrons with momentum of 250 MeV/c. If the setup will allow us to remove the heavy shielding we might be able to identify the relativistic particle peak in the triple coincidence time distributions. Even if we can get the time calibration from that peak it still worth taking a short run with d(e,ep+n) to make sure that the system is working well and to help understand the data.

3.4 Estimate of Singles Counting Rates and Accidental Coincidence Rates

counting rates are for:

- Incident beam energy of 4 GeV/c.
- Nuclear luminosity of $6 \times 10^{36} cm^{-2} sec^{-1}$
  corresponding to 100 μA beam, a 1 mm thick C target
- HRSe : 23 deg, 3.25 (±4.5%) GeV/c, solid angle: 6 msr
- HRSp : 40 deg, 1.25 (±4.5%) GeV/c, solid angle: 6 msr

- BigBite: 90 deg, 0.25-0.60 GeV/c, solid angle 96 msr
- n-array which is 4 layers of 10 160x10x10 cm^3 plastic scintillators covering 1.6x1m^2 at a distance of 6m from the target. Line of sight shielding: 2 inches of lead.
- The resolving time between HRSe and HRSp is 2 ns. The resolving time between the HRSe - HRSp coincidence and BigBite or the n-array is 5 ns. Notice that these are not the online time gates but will be obtained after calculated corrections.

3.4.1 Singles Rates

Table 3.5

HRSp	HRSe	neutron-array	BigBite
18KHz [1]	75Hz[2]	3 MHz [3]	8 MHz [4]

[1] - based on calculation of (e,p) and (e,π^+) with the computer code EPC of Lightbody and O'Connell. (e,p) singles rate is (14KHz) and (e,π^+) singles rate is (4Hz).

[2] - based on calculation of (e,e') and (e,π^-) with the computer codes QFS of Lightbody and O'Connell. The (e,π^-) rate is negligible.

[3] - singles rate for a bar (section 3.2) 120 kHz. For neutrals the rate for the whole array is: 10x0.9x120 (second layer)+10x0.8x120 (third)+10x0.7x120(4th)= 3 MHz.

[4] - based on calculation of (e,p) and (e,π^+) with the computer code EPC of Lightbody and O'Connell. The (e,p) and (e,π^+) rates are momentum dependent. We chose for this estimate the calculation at 400 MeV/c and used the full momentum bite of the spectrometer. 97% of this singles rate is due to (e,p). The EPC code is known to over predict proton inclusive yields at 90° and beyond. We are searching for data which can be used to better estimate these rates, but in the meantime are using the EPC values as a conservative worst case.

3.4.2 Double Coincidence Rates

The only double coincidence which is relevant for this measurement is the HRSe-HRSp $(e,e'p)$. The rest are relevant for accidentals estimate. So for all the others we do use upper limit which is equal to the singles rate on the less active arm in the coincidence. The real coincidence will be well below that of the upper limits.

Table 3.6

$(e,e'p)$ HRSe-HRSp	$(e,e'p)$ HRSe-BigBite	(e,en) HRSe-Array	(e,pp) HRSp-BigBite	(e,pn) HRSp-Array
0.014Hz[5]	$\ll$40Hz[6]	$\ll$40Hz[6]	$\ll$14KHz[7]	$\ll$14KHz [7]

[5] For the purpose of estimating the counting rate we assumed that at the selected kinematics all counts are due completely to 2N SRC. Using the cross sections from table 3.2 we get for both (pp) and (np) pairs and for the 350 MeV/c setup:

$\frac{d\sigma}{dE_e d\Omega_e d\Omega_p}$=(3.2)*(1+1/3)= 4.3 pb/MeV/sr^2

We did assumed a ratio $(p,p)/(p,n) = 1/3$. With the solid angles and energy range specify in section 3.3 of the proposal this lead to a coincidence rate of:

$4.3(10^{-12})(10^{-24})(6\ 10^{36})(6\ 10^{-3})(6\ 10^{-3})(20)$= 0.014 Hz

[6] This is an upper limit based on the singles rate of the HRSe [2]. We assumed that the rate for (e,e'p) equal the rate for (e,e'n) and equal half of the rate for (e,e').

[7] This is an upper limit based on the proton singles rate of the HRSp [1].

3.4.3 Triple Coincidence Rates

Table 3.7

(e,epn)	(e,epp)
2.2 10^{-3} [8]	1.25 10^{-2} [9]

[8] see Table 3.4 8/3600=2.2 10^{-3}

[9] see Table 3.4 45/3600=1.25 10^{-2}

3.4.4 Double Coincidence Random Rates

Table 3.8

$(e,e'p)$ HRSe-HRSp	$(e,e'p)$ HRSe-BigBite	(e,en) HRSe-Array	(p,p) HRSp-BigBite	(p,n) HRSp-Array
7.5 10^{-6}Hz [10]	NR	NR	NR	NR

[10] based on [1] and [2]: (14K)(75)(2 10^{-9})=2 10^{-3}

for $(e,e'p)$ the rand/real ratio is : 2 10^{-3}/0.014=0.14 (14%)

This singles rates were calculated within the full momentum bites of both HRSe and HRSp.

3.4.5 Triple Coincidence Random Rates

()-total (real) -random

Table 3.9

$(e,e'p)$n (HRSe-HRSp) Array	$(e,e'p)$p (HRSe-HRSp) BigB	(e,en)p (HRSe-Array) HRSp	$(e,e'p)$p (HRSe-BigB) HRSp
2.1 10^{-4} Hz [11]	5.5 10^{-4} Hz [12]	$\ll 10^{-3}$ Hz [13]	$\ll 10^{-3}$ Hz [13]

(p,n)e HRSe	(p,p)e HRSe
$\ll$2 10^{-3} Hz [14]	$\ll$2 10^{-3} Hz [14]

[11] - Using [5] and [3] (0.014)*(3*10^6)(5*10^{-9})=2.1 10^{-4}
[12] - Using [5] and [4] (0.014)*(8*10^6)(5*10^{-9})=5.5 10^{-4}
[13] - Using [6] and [1] (40)*(14K)(2*10^{-9})$\ll 10^{-3}$
[14] - Using [7] and [2] (75)*(14K)(2*10^{-9})$\ll$2 10^{-3}
rand/real rates for the triple coincidence are:
for $(e,e'pn)$ using [8,11,13,14] (2.1 10^{-4}) /(2.2 10^{-3})=10%
for $(e,e'pp)$ using [9,12,13,14] (5.5 10^{-4})/(1.25 10^{-2})=4.5%

3.4.6 Conclusion

Based on Table 3.4 in section 3.3 the enclosed is the expected real and random triple coincidence events.

Table 3.10

Pm [MeV/c]	total np real counts	total np random counts
300 $\pm$ 25	1800	180
350 $\pm$ 25	1200	120
400 $\pm$ 25	675	70
600 $\pm$ 50	300	30

Table 3.11

Pm [MeV/c]	total pp real counts	total pp random counts
300 $\pm$ 25	10500	470
350 $\pm$ 25	6750	300
400 $\pm$ 25	4500	200
600 $\pm$ 50	1800	80

The rates in Tables 3.10 and 3.11 were calculated assuming full correlation, i.e each large missing momentum $(e,e'p)$ event has a SRC partner. We will now use the calculated random rates to estimate the sensitivity of the measurement. If we cannot identify protons (neutrons) above the background in BigBite (n-array) we will check what is the consequence of that in terms of the $(e,e'pp)/(e,e'p)$ and the $(e,e'pn)/(e,e'p)$ ratios. Excess of counts above the background below five times the standard deviation of the background will be used for setting upper limits only. These upper limits are shown in Table 3.12.

Table 3.12

Pm [MeV/c]	upper limit to $(e,e'pp)/(e,e'p)$	upper limit to $(e,e'pn)/(e,e'p)$
300 ± 25	1.0%	4.%
350 ± 25	1.5%	5.%
400 ± 25	1.6%	6.%
600 ± 50	2.5%	9.%

Even if we will not be able to find real triple coincidences $(e,e'pp)$ or $(e,e'pn)$ events we can establish a meaningful upper limit for the SRC contributions to the large missing momentum tail of the $(e,e'p)$ reaction. These will be less than $\sim 2\%$ for the pp contribution and less than $\sim 10\%$ for the pn contribution.

3.5 Requested Beam Time

The counting rates that are presented in Tables 3.3 and 3.4 lead to the following beam time request:

- Set up, establishing coincidences, calibrations, background checks: **100 hours**
- Measurements at $Q^2 = 2$ (GeV/c)^2 with 3 different central momentum.

  For SRC dominance we expect about 4,000 (np) and 15,000-30,000 (pp) events in the $p_m = 300 - 600$ MeV/c region. This will allow us to the determine the SRC contribution with a statistical accuracy of better than 6% (at the highest $(600 \pm 50$ MeV/$c)$ missing momentum bin). If SRC events will not be observed we can set an upper limit on the SRC contribution at the level of about 2% for the (pp) pairs and 10% for the (np) pairs. The kinematics are given in Fig.7 and the experimental setup (3 spectrometers and a n-array) is in Fig.11. **450 hours**
- *TOTAL REQUESTED BEAM HOURS:* **550 hours**

3.6 Radiatiive Corrections

Radiative effects are an issue in every electron scattering experiment. In our case, we can look at it from two viewpoints.

- The trigger is an $(e, e'p)$ event. In this sense, we are dealing with similar issues to the ones which exist in every $(e, e'p)$ experiment, with two exceptions:

  1. This experiment is not looking for an absolute (differential) cross-section measurement.

  2. This is not a high resolution experiment.

  We are after the fraction of events in which there is a correlated proton or neutron with the $(e, e'p)$ event. As such, the radiation effects are not problematic.

- It is true that the determination of p_m in the (e,e'p) event is affected by the radiation. However, this is a small effect compared, for example, to the smearing of the "back-to-back" signal due to the CM motion of the correlated pair. What the radiation will do is "skew" this smearing to a small extent, which will not pose any problem.

3.7 Resources

We summarize here the special resources needed for the experiment. These are in addition to the "standard" hall A equipment for operating the two spectrometers, the beam and the target.

- 1. BigBite - The overall coordination, responsibility, effort and resources involved in installing a new third spectrometer in the hall is beyond the scope of this specific proposal. It depends on JLab, in particular the Hall A personal. The UVA group which has already started restoring the BigBite will provide commisioning support. The Glasgow group will be providing a new trigger detectors, replacing the present unsegmented scintillator layer. The money for this is available from their resources. Pending approval of this proposal, funding from the the Israeli Science Foundation is available to the Tel Aviv group to build a third layer of split ΔE counters.

- 2. neutron counters - The counters are available from KSU, UVa and Tel Aviv University.

- 3. veto counters - The detectors are available from KSU.

- 4. frame - will be built by KSU and TAU.

- 5. shielding - with JLab shielding blocks.

- 6. cables - We will need about 60 signal cables for the neutron counters. We also need about the same number of high voltage cables between the power supplies and the counters.

- 7. power supplies - (60 channels) most likely to be supplied by KSU.

- 8. fast electronics - each of the detectors has 2PMT's. The signals will go to CFD's. There will also be several veto counters. We have the necessary CFD's. We also have the NIM units for the hardware trigger logic. The two PMT's on each plastic bar are operated in coincidence after which all counters are also OR'ed. Thus, just one single signal will announce a hit in the third arm counter which can then be used to create a triple coincidence with a quasi-free event in the $(e, e'p)$ reaction. However, no signals from the third arm counters will be used in the hardware trigger.

- 9. Readout electronics: There will necessarily be changes to the "standard" DAQ in order to read and record the extra information from the BigBite spectrometer. We will also have to read approximately 60 TDC signals for the neutron counter array.

- 10. Manpower: The group has much experience in :

  $(e, e'p)$ measurements

  triple coincidence measurements

  neutron detection

  The group is sufficiently large and experienced to perform the proposed experiment. We would have to emphasize that the addition of the BigBite spectrometer to hall A is a major change that will require participation and responsibility of the hall A personnel.

Appendix I The $A(p, 2p + n)$ Experiment at BNL

This proposed experiment is to some extent a follow up of an $A(p, ppn)$ measurement we performed at BNL. The experiment (E850) was performed at the AGS accelerator at Brookhaven National Laboratory with the Exclusive Variable Apparatus (EVA) spectrometer [86, 87, 88, 89].

The high-momentum transfer quasi-elastic ^{12}C$(p, 2p)$ reaction was measured near 90° c.m. for 6 and 7.5 GeV/c incident protons, in a kinematically complete coincidence experiment. The three-momentum components of both high p_t final state protons were measured. The setup is drawn in Fig. I.1. It shows the solenoidal cryogenic magnet with an axial field in the direction of the beam, entering from the left. The beam hit targets located near the center of the magnet and the two emerging protons were measured in a series of detectors.

Great care was taken to ensure the quasi-elastic scattering nature of the events. A small excitation energy of the residual nucleus ($E_{\rm miss}$) was imposed in order to suppress events where additional particles could be produced in the process. Inelastic events that leaked into the data were subtracted. The procedures and results are described in Mardor et al. [90, 88]. In Fig. I.2 we show the distributions of p_{fz} which is is the missing mementum component parallel to the beam direction. The component p_{fz} is the component parallel to the beam direction and p_{fy} is one of the transverse components. The momenta were measured up to 250 MeV/c per component, (about 430 MeV/c for the total momentum). Also in Fig. I.2 , we compare the measured momentum distributions to a simple independent particle Fermi motion distribution. An harmonic oscillator (HO) was used with parameters fitted to C from electron scattering data [91]. The HO calculation and the data in the figure are normalized to 1000 at the first bin. As is well known and can be seen clearly, the independent particle model fails substantially to describe the large momentum tails of the distribution. It seems that one is forced to invoke some short range correlation contributions.

In the same experiment, in addition to the quasi-elastic C(p,2p) reaction, we also measured the emerging neutrons . Referring back to Fig. I.1, we see at the bottom a series of scintillation counters which measured the neutron momenta by Time Of Flight (TOF). The neutrons were detected in coincidence with the two emerging high momentum protons. Below the targets we placed a series of 16 scintillation bars covering an area of 0.8×1.0m^2 and 0.25 m deep. They spanned an angular range of 102 to 125 degrees from the target. The TOF resolution of $\sigma = 0.5$nsec corresponds to a momentum resolution of $\sigma = 30$ MeV/c at the highest momentum. A set of veto counters served to eliminate charged particles. Lead sheets were placed in front of the veto counters in order to reduce the number of photons entering the TOF spectrum. A clearly identified peak at about 3 nsec per meter flight path, due to remaining photons from the targets, was used for calibration and to measure the timing resolution. We applied a cutoff in the TOF spectrum at 6 nsec per meter flight path, keeping neutrons below 600 MeV/c, in order

to eliminate any photons.

We had a very successful second data taking period at the AGS of the Brookhaven National Laboratory, from July to December 31, 1998 after a rebuilt of the EVA spectrometer during 1996-8. Among other reactions we collected data on the reaction $^{12}C(p, 2p+n)$ at several bombarding energies. We analyzed the data at 5.9 GeV/c incoming momentum from the 1998 period. For this run the spectrometer was upgraded with the installation of two new neutron counter arrays which increased the acceptance for backward neutrons by a factor of 2.5 over the 1994 configuration. See Figure I.3 for the new 1998 experimental setup.

An example of a triple coincidence event which displays a NN SRC, is shown in Fig. I.4. We show the transverse components $\mathbf{p}_t(p_1)$ and $\mathbf{p}_t(p_2)$ of the two outgoing high momentum protons as they were reconstructed in the trajectory analysis. The transverse momentum component of the struck target proton $\mathbf{p}_t(p) = \mathbf{p}_t(p_1) + \mathbf{p}_t(p_2)$ and the component of the neutron on the plane perpendicular to the beam are drawn as well. If the struck proton was correlated with a nearby neutron and the pn pair is at rest, the neutron will emerge in the direction opposite to that of the struck proton and with the same magnitude $\mathbf{p}(n)$= - $\mathbf{p}(p)$. If the correlation is of short range nature, we also expect both $p(n)$ and $p(p)$ to be above the Fermi sea level.

Most of the events measured do not have these ideal characteristics. The angular correlation is spread out due to limited experimental resolution, to center of mass motion of the pn pair in the nucleus and to final state interactions (FSI) of the outgoing protons. Notwithstanding the inevitable smearing of the angular correlation, we can extract information on the np correlation from our data by relaxing somewhat the stringent "back to back" requirement. None of the above effects is sufficiently large to prevent us from determining whether the momentum of the target proton pointed upwards or downwards. All the neutrons are detected in the downward direction. Consequently, we concentrate on the vertical (up-down) component of the struck proton. In Fig. I.5 we plotted that component with respect to the *total momentum* of the neutron obtained from the 5.9 and 7.5 GeV/c beam momenta measurements at 1994 and the new 6 GeV/c data from 1998. Each data point represents a single measured event. The resolution of the vertical momentum component depends on the azimuthal angle of the pp scattering plane. The resolution is best for a horizontal scattering plane and worst for the vertical plane. The different sizes of the error bars in Fig. I.5 reflect this variation in the resolution.

Any proton with a vertical component in the downward direction cannot be a partner in the two-nucleon np correlation. We see that, up to a neutron momentum of $k_F \simeq$ 220 MeV/c, (see the vertical dashed lines in Fig. I.5) there are proton components in the downward as well as in the upward directions. Above that momentum there are very few downward pointing proton momenta and most point upwards. This is what one expects for correlated nucleon pairs. The large neutron momenta are associated with upward going protons while below the Fermi level, where the momenta can originate from the mean field, there is no preference.

The absence of downward pointing proton momenta at high neutron momenta, is a

clear indication of the dominance of two-nucleon correlations. We emphasize the fact that the conclusion is based on kinematics and does not depend on specific theoretical models.

A series of tests were performed to ascertain that the up/down asymmetry in Fig. I.5. is not an experimental artifact of the spectrometer or of analysis procedures. We looked for asymmetries in, (i) the double coincidence $(p, 2p)$ quasi-elastic scattering data, (ii) the triple coincidence data, where the third coincidence was taken from the photon peak in the neutron counter and (iii), we changed the $E_{\rm miss}$ region to $1.2 < E_{\rm miss} < 2$ GeV. We did not observe asymmetries in any one, or combinations, of these tests.

Final state interactions could, in principle, mimic this asymmetry. This can happen if one of the outgoing protons scatters elastically from a neutron in the same nucleus, at an angle such that the recoil neutron enters the neutron counters. The momentum transferred to the proton cannot be distinguished from the original momentum of the struck proton before the hard interaction. Since the neutron detectors are positioned at a backward angle, the probability for such a recoil neutron to enter the counters is very small. We estimated the FSI contribution to the events shown in Fig I.5. in the following way. We assumed that the FSI can be described by a Glauber-like calculation, as in Ref [74]. We simulated the geometry of the spectrometer and neutron detectors and determined the number of neutrons and their momenta that could contribute to Fig. I.5, for all the $(p, 2p)$ quasi-elastic events. The contribution of FSI to the events in Fig. I.3 is about 10%. The number of initial state interactions for the 6 GeV/c projectile, causing a neutron to recoil to an angle of 100 deg, is negligible.

In conclusion it is possible to identify two-nucleon short range correlations on an event by event basis. The identification is based on kinematical arguments. The measured events are associated with high momentum components of the nuclear wave function. It seems that high energy exclusive reactions are an effective tool for the study of SRC in nuclei and it should encourage further studies, such as high energy $(e, e'p + \mathrm{N})$ measurements.

We also analyzed the data at 5.9 GeV/c incoming momentum from the 1998 period looking at a sample of events which is an order of magnitude larger than the QE $(p, 2p)$ events. These events include neutrons emitted into the back hemisphere, in the laboratory system in (triple) coincidence with two emerging $p_t > 0.6$ GeV/c particles. We measured the momentum spectra of the backward going neutrons, which have the same universal shape observed in earlier (inclusive) reactions induced by hadrons, γ, ν, and $\bar{\nu}$ beams (See Fig. I.6).

We also integrated the spectra and determined the fraction of the hard scattering events which are in coincidence with at least one neutron emitted into the back hemisphere, with momenta above 0.32 GeV/c. (See Fig.I.7).

Contrary to the earlier measurements which found that only a small fraction (of the order of 10%) of the total inelastic cross section for light nuclei was associated with backward going nucleons, we found that about half of the events are of this nature. We speculate that the reason for the large difference is the strong total center of mass (s)

dependence of the hard reaction and short range nucleon correlations in nuclei.

The measurement covers a small kinematic corner of the inclusive proton-carbon cross section that we will refer to as in the *"kinematic vicinity of hard quasi-elastic scattering"* at 90° cm. This kinematic region is loosely characterized by the observation of two high transverse momentum (p_t) positively charged final state particles that carry away most of the beam energy. The two tracks are observed at large laboratory polar angles, back-to-back in the proton-proton (pp) center of mass (cm) frame, within a narrow range of the laboratory angles corresponding to pp scattering at 90°. This class of events is a superset of the quasi-elastic event sample in that angular range.

There are no models in the literature that have considered an increase in the backward neutron production for events in the "kinematic vicinity" of quasi-elastic scattering. However models that attempt to explain the universal inclusive results do exist.

One model [92, 46] has considered rescattering of initial or final state particles associated with a primary interaction and the spectator nucleons as the source for backward nucleons. We are not aware of any features of this new kinematic region that would cause a large enhancement of rescattered backward neutrons above that of other kinematic topologies.

The other approach [54, 93] is the one discussed earlier in this paper, that the backward neutron enhancement may indeed be associated with the two nucleon correlation picture. If an incident proton scatters elasticaly off of a single nucleon (QE process), because the proton-nucleon elastic cross section scales as $1/s^{10}$, it will preferentially scatter on nucleons in the nucleus which have large momentum in the direction of the incident particle (small s). It should be emphasized, that for this interpretation, QE scattering is not necessary, any hard process with strong s-dependence will result in the same phenomenon. If a strong s dependence in the cross section can be associated with events in this new region, then the two nucleon short range correlation picture could be naturally extended and applied to our new measurement.

Appendix II Parasitic ^{3}He$(e,e'p)$ Measurements in Hall A

Experiment 89-044 [22] is a measurement of ^{3}He$(e,e'p)$ that ran in Hall A from December 1999 through March 2000. In particular, part of E89-044 is aimed at the study of the high momentum components of ^{3}He using the $(e,e'p)$ reaction in perpendicular and parallel kinematics. During this experiment we made parasitic measurements of ^{3}He$(e,ep+n)$ using an array of scintillator bars to detect neutrons. The neutron bars were placed (See Fig II.1) to measure the correlated neutron recoiling against the initial high momentum proton. ("Back to back") The third nucleon in ^{3}He (proton) is a spectator assumed to be at rest in the nucleus. The ejected electrons and protons detected by E89044 in $(e,e'p)$ were used to tag the additional neutron in ^{3}He$(e,e'p+n)$. In the case of ^{3}He, this measurement is kinematically complete.

We first installed the neutron counters array on the proton arm side and measured two high missing momentum ($p_{\rm m}$) perpendicular kinematical points: $p_{\rm m}=300$ MeV/c ($\Sigma 2$ point 8 of E89-044) and $p_{\rm m}=425$ MeV/c ($\Sigma 2$ point 11 of the E89-044). For each point we also measured the complementary kinematics ($\Sigma 2$ points 7 and 10) where the neutron had the same $p_{\rm m}$ recoil away from our counters. It is worth noting that the missing momenta are for the two body breakup of ^{3}He. For the np back to back kinematics, the momenta of the nucleons in the pair are lower: 215 MeV/c for point 8 and 300 MeV/c for point 11.

We then moved the n detector array to the other side of the beam and measured in parallel kinematics one point (point 24 of E89-044) with $p_{\rm m}=300$ MeV/c. We also measured a point with $p_{\rm m}=0$.

Altogether we collected about 25 million triggers which are about half of the triggers that the host experiment (89-044) collected under these selected kinematical conditions. The data are being analyzed now.

Each PMT (there are two PMTs per counter) was connected to a multi-hit TDC with a range of 1.5μsec. A coincidence between the HRS$_e$ trigger signal and the HRS$_h$ trigger signal was used as a common stop to the TDCs. The data were collected in a parasitic mode completely without any modification to the standard hall A data stream. After we matched the events on the parasitic data files and the hall A files we had for each $(e,e'p)$ double coincidence event (hall A event type 5) a recorded history of 1.5μsec around that coincidence for each one of the PMTs in the neutron arry.

We request a hit in both left and right PMT of the same counter (the difference in left and right time was limited to a known window). We then identified the neutrons as those hits in which a counter (both left and right) fired but none of the three counters in front of it fired. We therefore used only three out of the four walls of counters. The front wall was used as a veto only. We had 5-7 "neutrons" per event which yield an average of about 0.3 "neutrons" per counter per $(e,e'p)$ double coincidence event.

We applied software cuts to select "good" candidates for the $(e,e'p)$ events. The major cut used was on the time of the electron and proton emerging from the target as calculated based on the spectrometer time measurements and corrections for the particle

travel in the spectrometers. In Fig II.2 we show a typical e-p time distribution for a measured point with a random coincidence rate relatively high (point 11) and low (point 8). We also applied cuts that select events from the target and not its wall, identify the particle in each spectrometer and made the electron and proton vertex consistent. With these cuts the missing energy of the $(e, e'p)$ double coincidence events is shown in figure II.3 a and b for points 8 and 11 respectively. To produce each one of these missing energy spectra we subtracted from the events in the e-p coincidence peak events that correspond to half the size of the time window earlier and half after the real coincidence time.

For the selected $(e, e'p)$ events in the missing energy range of 10-80 MeV we look at the TOF distributions of the neutrons detected up to 1.5 μsec before the coincidence signal time. The TOF was reconstructed from the sum of the TDCs (left and right) for each identified "neutron". The obtained distributions, dominated by random coincidences, have exponential shape as shown in figure II.4.

For this parasitic measurement we could not measure a $d(e, ep + n)$ to determine the position of the TOF peak that corresponds to known momentum neutrons. We rather measured the cables length and did some estimate that lead us to the conclusion that the 200-500 MeV/c neutrons should be somewhere between channels 650-850 on the plotted distributions of TOF.

We simulated the expected signal if it had 200 or 500 events on top of the measured exponential background. For the simulation we assumed that the signal is a Gaussian with width of 30 nsec center at channel 800. The simulations are shown in figure II.5 for diffent background levels. As can clearly seen in these figures, a signal of about 500 events should be able to be identified clearly. A measured TOF distribution for point 11 is shown in figure II.6. The calculations used to obtain the count rates for this proposal (see section 3.3) gives an expected yield of 180 neutrons in the 10hr measurement of point 11. This prediction is consistent with the measurement. It can be seen that a peak correspond to 500 events was not found. The lack of a clearly seen peak of 500 events or more can be translated to an upper limit on the ratio of $(e, ep+n)/(e, ep)$. If we assume that the neutron array covered about $50-70\%$ of the solid angle of the correlated neutrons with a detection efficiency of 35% and that the transmission of neutrons in the lead and the first scintillator wall (used as a veto) was 50% and 90% respectively, we get that each detected neutron is one out of 11 emitted correlated neutrons. Therefore, a peak of 500 neutrons will correspond to about 5500 neutrons. We found about 15,000 $(e, e'p)$ double coincidence events in both points 8 and 11 so this correspond to a ratio of 5500/15000=35%. The fact we definitely do not see such signal above the background mean an upper limit on the $(e, ep + n)/(e, ep)$ of less than 35% for missing momentum of 300 MeV/c. This is a preliminary analysis, more careful work is still required to reach final conclusion.

The calculations used to obtain the count rates for this proposal (see section 3.3) gives an expected yield of 180 neutrons in the 10 hour measurement of point 11. This prediction is consistent with the measurement. For this proposal we expect yields of 300-2000 with a signal to noise ratio which is a factor of 4 better than the one we had

in the parasitic run. We also will know exactly were to look for the neutrons using the $d(e, e'p)$ calibration.

References

[1] E.Piasetzky, W.Bertozzi, J.Watson, S.Wood *(spokespersons).*, *Studying the internal small-distance structure of nuclei via the triple coincidence* $(e, e'p+\mathrm{N})$ *measurement.* Experiment 97-106 Proposal to Jefferson Laboratory, 1997 (unpublished).

[2] C. Ciofi degli Atti, E. Pace and G. Salme, Phys. Rev. **C21**, 805 (1980).

[3] O. Benhar, A. Fabrocini and S. Fantoni, Nucl. Phys. **A505**, 267 (1989).

[4] C. Ciofi degli Atti, L. Frankfurt, S. Simula and M. Strikman, Phys. Rev. **C44** 7 (1991).

[5] V.Pandharipande, I.Sick and P.K.A. de Witt Huberts, Rev. Mod. Phys. 69(1997), 981.

[6] D.B.Day *et al.*, Phys.Rev.Lett. 59, 427 (1987).

[7] J. Arrington, *et al.*, Phys. Rev. Lett. 82, 2056 (1999).

[8] L. L. Frankfurt, M. I. Strikman, D. B. Day and M. M. Sargsyan, Phys. Rev. **C48**, 2451 (1993).

[9] O. Benhar,et al. Phys.Rev.C47(1993),2218.

[10] J. S. O'Connell et al., Phys. Rev. Lett. **53**, 1627 (1984); Phys. Rev. **C35**, 1053 (1987).

[11] W.Bertozzi, R.W. Lourie and E.J. Moniz, in Modern Topics in Electron Scattering, (World Scientific, 1991), B.Frois and I.Sick eds.

[12] P.E.Ulmer *et al.*, Phys. Rev. Lett. 59, 1159 (1987).

[13] J. Koch and N. Ohtsuka, Nucl. Phys. **A435**, 765 (1985).

[14] G.van der Steenhoven *et al.*, Nucl.Phys. A484, 445 (1988).

[15] L. Lapikas et at., Phys. Rev. C61 (2000) 064325.

[16] A. Saha, W. Bertozzi, R. W. Lourie, and R. B. Weinstein, JLAB proposal 89-003, 1989; see also K.G. Fissum, MIT-LNS Internal Report #02, 1997 and `http://www.jlab.org/~fissum/e89003.html`

[17] J. Gao *et al.*, Phys. Rev. Lett. **84**, 3265 (2000).

[18] N. Liyanage *et al.*, to be submitted to Phys. Rev. Lett. in 2000.

[19] J. J. Kelly, Phys. Rev. **C60**, 044609 (1999).

[20] J. M. Udias *et al.*, Phys. Rev. Lett. **83**, 5451 (1999).

[21] L. Frankfurt, M. Strikman, M. Zhalov http://arXiv.org/abs/hep-ph/0011088.

[22] M.B Epstein, R.W. Lourie, J. Mougey, A. Saha *(spokespersons)*, CEBAF proposal 89-004, 1989.

[23] *(spokespersons)*, JLab proposal 97-111, 1997;

[24] J.M. Le Goff et al., Phys. Rev. **C50** 2278 (1994).

[25] C. Marchand, et al., Phys. Rev. Lett. **60**, 1703, (1988).

[26] J.J. van Leeuwe, et al., *Talk given at the 15th International Conference on Few-Body Problems in Physics (FB 97), Groningen, Nederlands, 22-26 Jul 1997.* nucl-ex/9709007.

[27] R.Ent *et al.*, Phys. Rev. Lett. 62, 24 (1989).

[28] C.J.G.Onderwater *et al.*, Phys. Rev. Lett. 78, 4893 (1997).

[29] L.J.H.M.Kester *et al.*, Phys. Rev. Lett. 74, 1712 (1995).

[30] C.J.G. Onderwater et al. Phys. Rev. Lett. 81 (1998) 2213.

[31] A.Zondervan *et al.* Nucl. Phys. A587, 697 (1995).

[32] D.L. Groep et al., Phys. Rev. Lett. 83 (1999) 5443.

[33] D.L. Groep et al., nucl-ex/0008008 and to appear in Phys. Rev. C63, January 2001.

[34] K.I. Blomqvist et al., Phys. Lett. B 424 (1998) 71.

[35] G. Rosner, rogr. Part. Nucl. Phys. 44 (2000) 99.

[36] J.Arends *et al.*, Z.Physik A298, 103(1980).

[37] M.Kanazawa *et al.*, Phys.Rev. C35, 1828 (1987).

[38] J. Ryckebusch, S. Janssen, W. Van Nespen and D. Debruyne, Phys. Rev. C 61 (2000),1.

[39] Stijn Janssen, Jan Ryckebusch, Wim Van Nespen and Dimitri Debruyne, Nucl. Phys. A672 (2000), 285-309.

[40] L. Weinstein et al., cont. BB4 to the DNP 2000 meeting, October 2000, Williamsburg, Virginia.

[41] R. Niyazov et al., cont. BB5 to the DNP 2000 meeting, October 2000, Williamsburg, Virginia.

[42] B. Zhang et al., cont. BB9 to the DNP 2000 meeting, October 2000, Williamsburg, Virginia.

[43] G.A. Leksin in Proceeding of the XVIII International conference on High Energy Physics, Tbilisi, 1976, ed. N. N. Bogolubov et al.

[44] Yu.D. Bayukov *et al.*, Sov. J. Nucl. Phys. 18 (1974) 639; Sov. J. Nucl. Phys. 42 (1985) 116, and 238; Sov. J. Nucl. Phys. 34 (1981) 437.

[45] Yu.D. Bayukov *et al.*, Sov. J. Nucl. Phys. 41 (1985) 101; ITEP-5-1985 (1985) 67.

[46] V.I. Komarov *et al.*, Nucl. Phys. A326(1979)297.

[47] S. Frankel *et al.*, Phys. Rev. Lett. 36 (1976) 642.

[48] K.V. Alanakyan *et al.*, Sov. J. Nucl. Phys. 25 (1977) 292.

[49] There are new, not yet published, data from Hall B at JLab, K. Sh. Egiyan, private communication.

[50] M.R. Adams *et al.*, Phys. Rev. Lett. 74 (1995) 5198.

[51] J. P. Berge *et al.*, Phys. Rev. D18 (1978) 1367.

[52] V.I. Efremenko *et al.*, Phys. Rev. D22 (1980) 2581.

[53] E. Matsinos *et al.*, Z. Phys. C44 (1989) 79.

[54] L.L. Frankfurt and M.I. Strikman, Phys. Rep. 76 (1981) 214; *ibid*, 160 (1988) 235.

[55] Yu D.Bayukov *et al.*, Sov. J. Nucl. Phys. 42, 116 (1985), and 238; Sov. J. Nucl. Phys. 34, 437 (1981).

[56] K. Egiyan et al., submitted to Physics of Atomic nuclei, 1997.

[57] K. Egiyan et al., cont. BB8 to the DNP 2000 meeting, October 2000, Williamsburg, Virginia.

[58] J. Aclander *et al.*, Phys. Lett. B453 (1999) 211.

[59] D. Day and B. Filippone (spokespersons), CEBAF proposal E89-008.

[60] J. Zhao (spokesperson), JLab proposal E-97-011.

[61] K. Egiyan (Spokesperson), CEBAF proposal E-89-036.

[62] S. E. Kuhn and K. A. Griffioen (spokespersons), CEBAF proposal E-94-017.

[63] H. Baghaei (spokesperson), CEBAF proposal E-89-015.

[64] V. Gavrilov and G. Leksin (spokespersons), CEBAF proposal E-89-032.

[65] G. R. Farrar *et al.*, Phys. Rev. Lett. 62 (1989) 1095.

[66] R. J. Glauber, in *Lectures in Theoretical Physics*, edited by W. Brittain and L. G. Dunham, Wiley Interscience, New York, **V.1**(1959).

[67] E.J. Moniz and G.D. Nixon, Annals of Physics **67** 58 (1971).

[68] D.R. Yennie in *Hadronic Interactions of electrons and Photons* ed. J. Cummings, D. Osborn, 321 (1971).

[69] L. L. Frankfurt, M. M. Sargsyan and M. I. Strikman, Phys. Rev. **C56**, 1124 (1997).

[70] L. L. Frankfurt, W. G. Greenberg, J. A. Miller, M. M. Sargsyan and M. I. Strikman, Z. Phys. **A352**, 97 (1995).

[71] M.M. Sargsyan, "Event generator of electron-nucleus reactions", CLAS NOTE 92-018, 1992.

[72] K.Sh. Egiyan, M.M. Sargsyan, "Cross-Section of Electron - Off-Shell Nucleon Interaction" CEBAF-PR-93-001, (1993).

[73] T. de Forest, Nucl Phys. **A392**, 232 (1983).

[74] I. Mardor *et al.*, Phys. Rev. C46, 761 (1992).

[75] R. G. Arnold et al., Phys. Rev. **C42** (1990),R1.

[76] J. M. Laget, Phys. Lett. **B199**, 493 (1987).

[77] A. Bodek *et al.*, Phys. Rev. D20, 1471 (1979).

[78] D. Geesaman (spokesperson), CEBAF proposal E-91-013.

[79] D.J.J. de Lange *et al.*, Nucl. Instrum. Meth. A 406 (1998) 182 - 194.

[80] D.J.J. de Lange *et al.*, Nucl. Instrum. Meth. A 412 (1998) 254 - 264.

[81] http://erwin.phys.virginia.edu/research/groups/thirdarm/.

[82] R. Cecil, B.D. Anderson, R. Madey, Nucl. Inst. and Meth. 161, (1979) 439.

[83] M. Sargsyan, private communication.

[84] S. Turck-Chieze, P. Barreau, et al., Phys.Lett.142B(1984),145.

[85] T. de Forest, Nucl Phys. **A392**, 232 (1983).

[86] M.A.Shupe *et al. EVA, a solenoidal detector for large angle exclusive reactions: Phase I - determining color transparency to 22 GeV/c.* Experiment E850 Proposal to Brookhaven National Laboratory, 1988 (unpublished).

[87] *Measurement of the dependence of the $C(p, 2p)$ cross section on the transverse component of the spectral momentum*, S.Durrant, PhD thesis, Pennsylvania State University, 1994 (unpublished).

[88] *Quasi-Elastic Hadronic Scattering at Large Momentum Transfer*, Y.Mardor, PhD thesis, Tel Aviv University, 1997 (unpublished).

[89] J.Y.Wu *et al.* , Nuclear Instruments and Methods A 349 (1994) 183.

[90] Y.Mardor *et al.*, Phys. Lett. B453(1999), 211.

[91] M. Sargsyan, private communication, and H. Bidasaria et al. Nucl. Phys. A355, 349 (1981).

[92] V.B. Kopeliovich, Sov. J. Nucl. Phys. 26 (1977) 87.

[93] L.L. Frankfurt and M.I. Strikman, Phys. Lett. B69 (1977) 93.

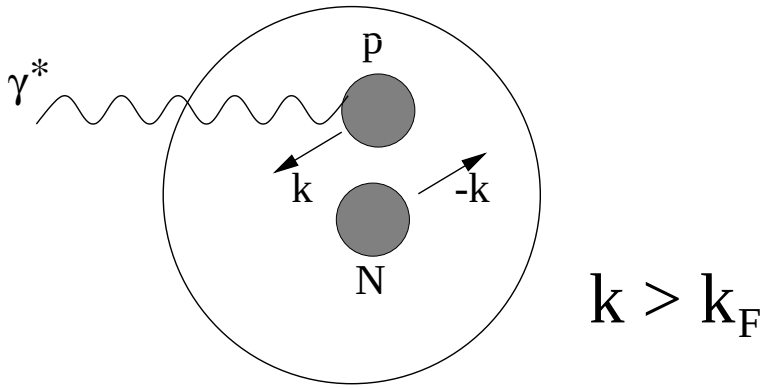

Figure 1: Breakup of NN SRC in the nucleus induced by a virtual photon.

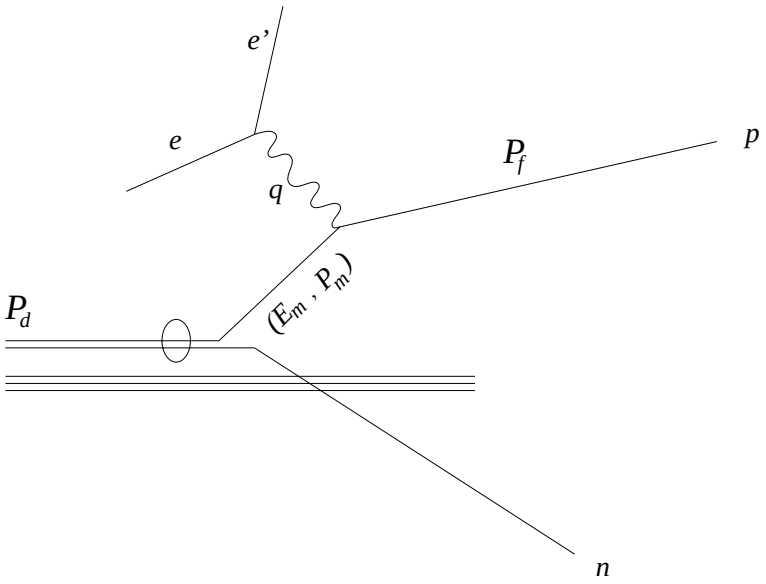

Figure 2: Diagram for the quasi-elastic breakup reaction of a pair at rest in the nucleus. The kinematical variable are defined in the text.

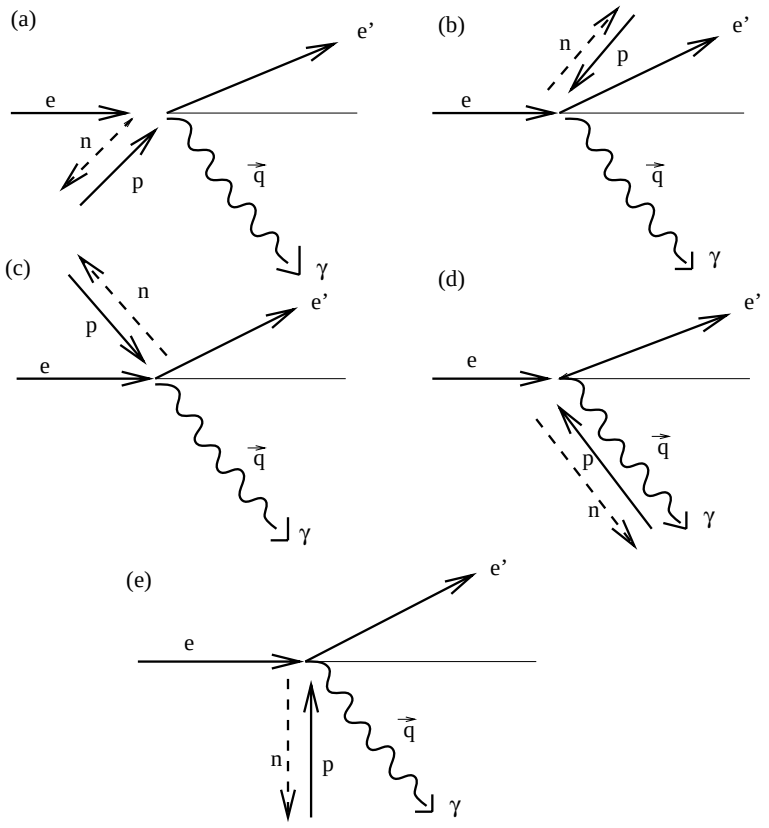

Figure 3: Relative geometry between the target proton momentum and the incident virtual photon momentum $\vec{q}$. a,b- perpendicular, c-parallel, d-antiparallel, e-'almost anti-parallel'.

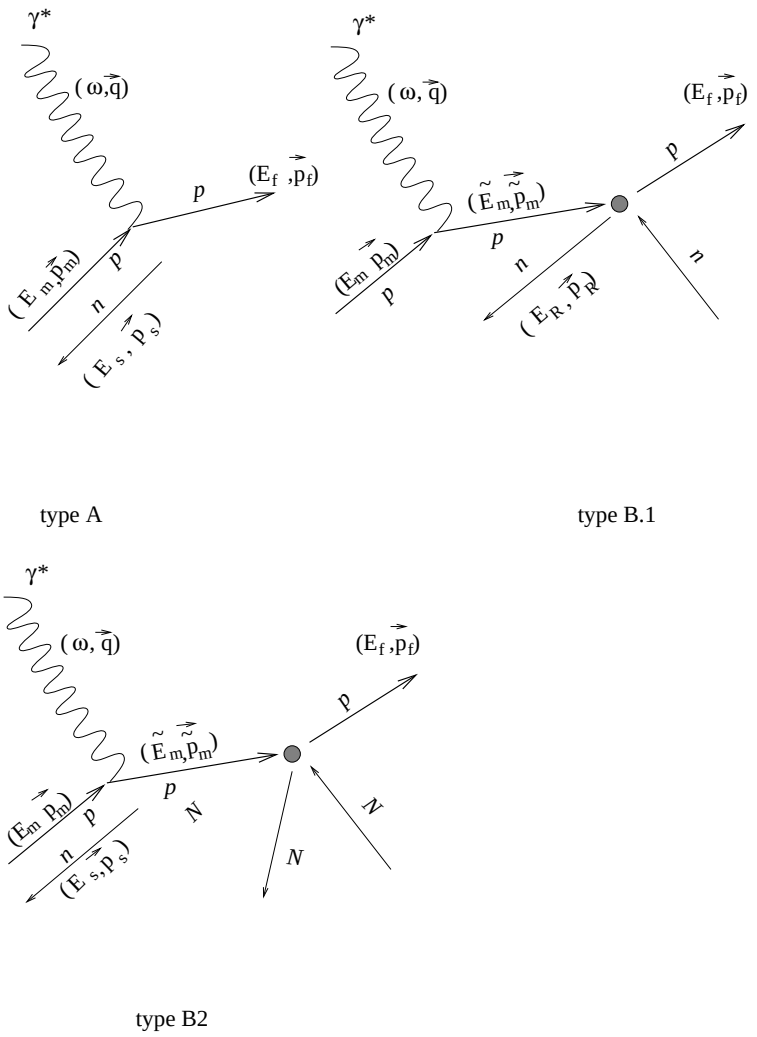

Figure 4: Diagrammatic presentation of QE (type A) events and rescattered (type B) events.

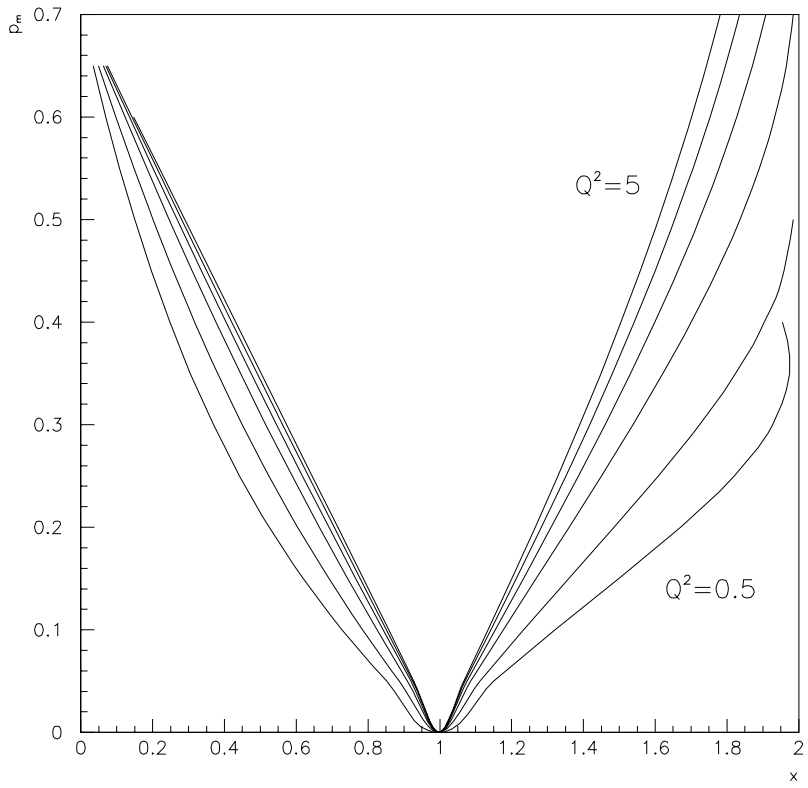

Figure 5: The x dependence of missing momentum p_m (in (GeV/c)) probed in $(e, e'p)$ reaction at different Q^2 = (0.5, 1, 2, 3, 4 5 $(rmGeV/c)^2$). The momentum of of the final proton $\vec{p}_f$ is parallel to $\vec{q}$.

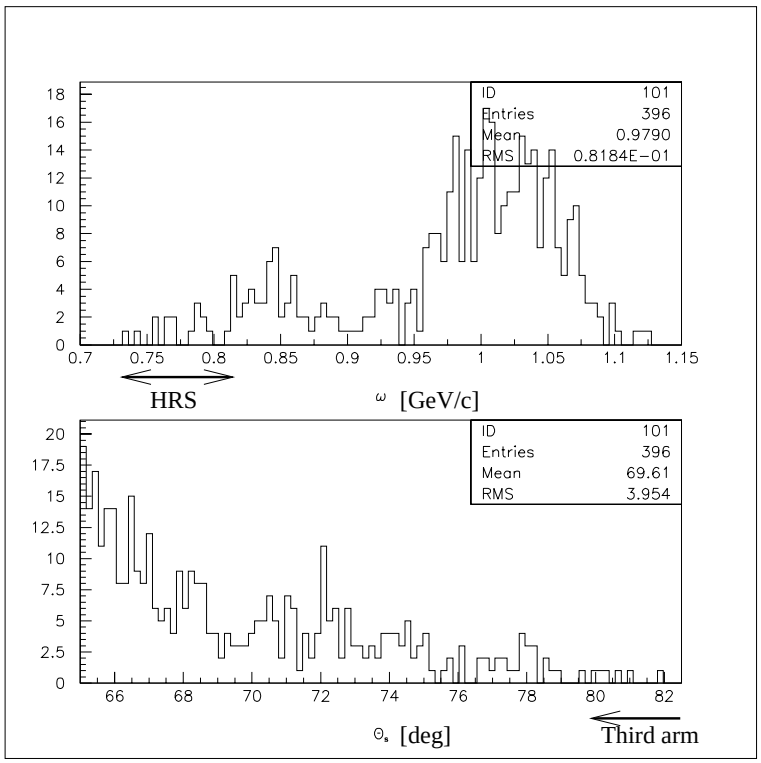

Figure 6: Transferred energy distributions (ω) and neutron recoil angles (θ_s) for the Δ production follow by rescattering events. The experimental acceptances are also shown.

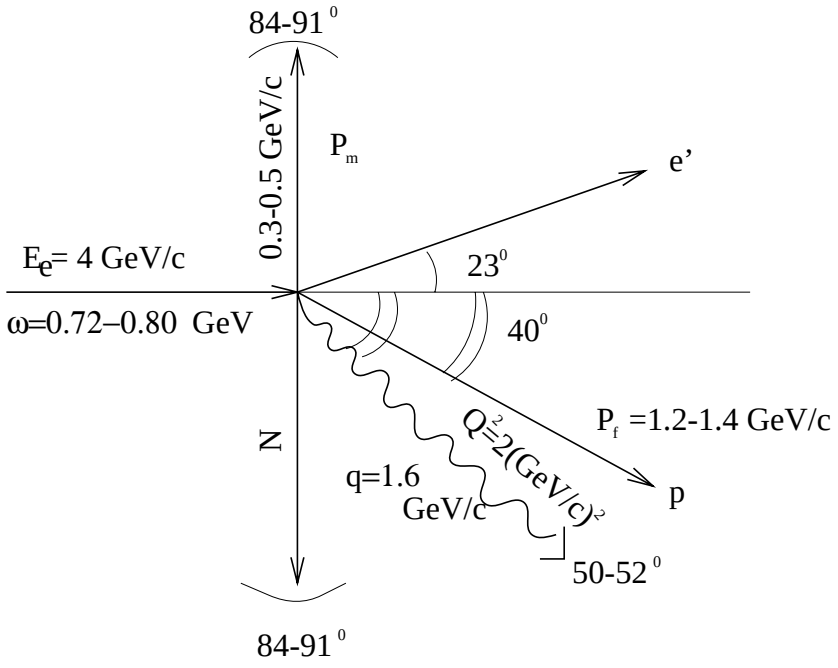

E_e =initial electron energy = 4 GeV

θ_e = scattered electron angle = 23^0

θ_N = spectator angle = 85^0

ϕ_N = azimuthal angle of spectator nucleon = 180^0

ω	q	Q^2	x	θ_q	P_f	E_m	P_m	θ_p	ϕ_p
GeV	GeV/c	$(GeV/c)^2$		deg	GeV/c	GeV	GeV/c	deg	deg
0.73	1.62	2.08	1.52	52.23	1.21	0.14	0.52	38.80	180.0
0.80	1.64	2.01	1.36	49.86	1.41	0.04	0.29	43.16	180.0

Figure 7: Kinematics for the reaction $(e, e'p + n)$ in "almost-parallel geometry" at $Q^2 = 2.0$ $(\mathrm{GeV}/c)^2$. The variables are defined in the text. The table shows the values of these variables for two missing momenta $p_m = 300$ and 500 MeV/c within the proposed range $(p_m = 300 - 600$ MeV/$c)$.

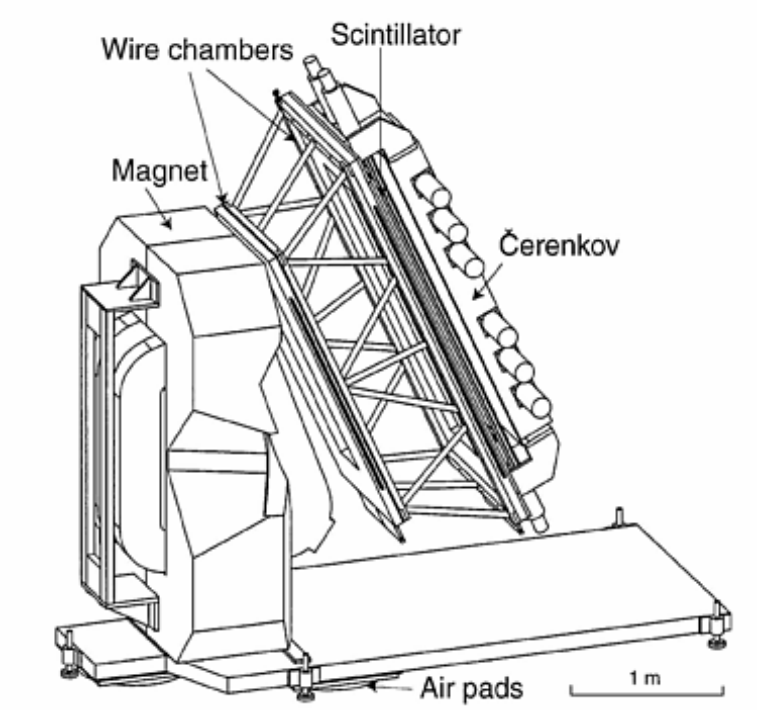

Figure 8: An artist's view of the BigBite spectrometer showing the magnet and the detector system.

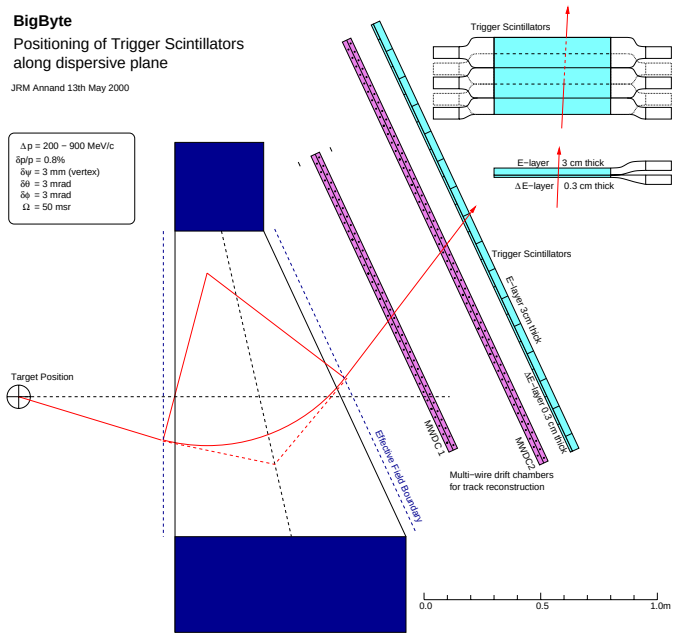

Figure 9: Schematic of the BigBite spectrometer showing the new trigger scintillators proposed by the Glasgow group. Figure, courtesy of John R.M. Annand

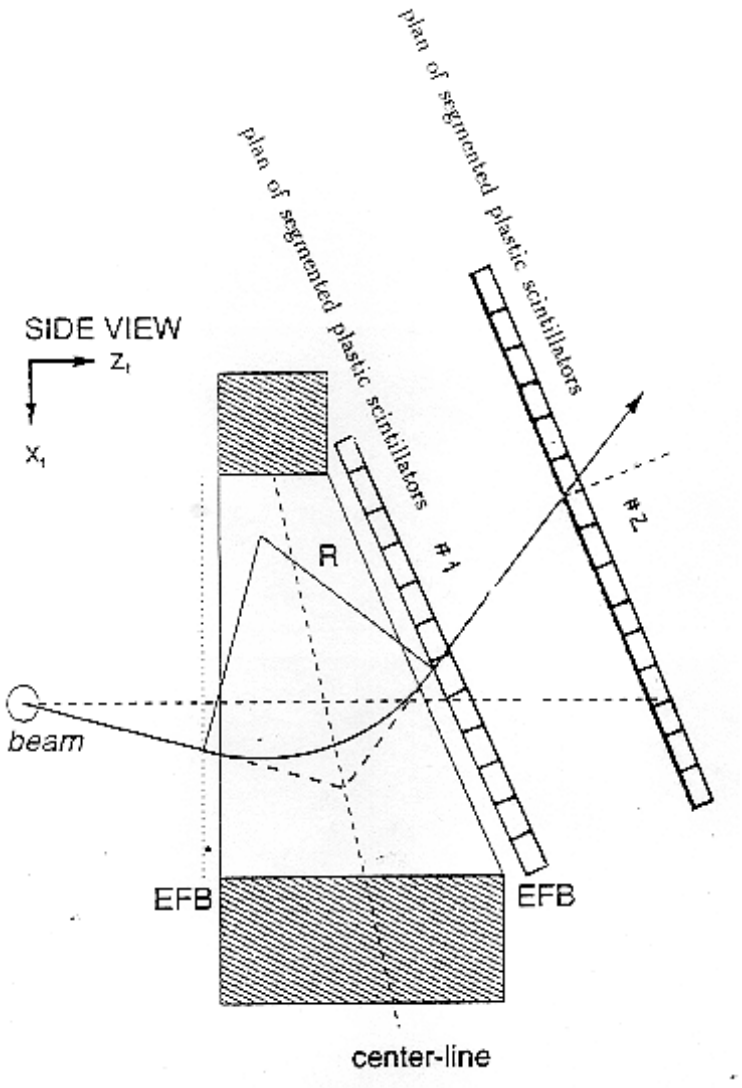

Figure 10: Schematic of the BigBite spectrometer showing the proposed scintillator setup. TOF will be measured between scintillator planes 1 and 2. EFB stands for effective field boundary.

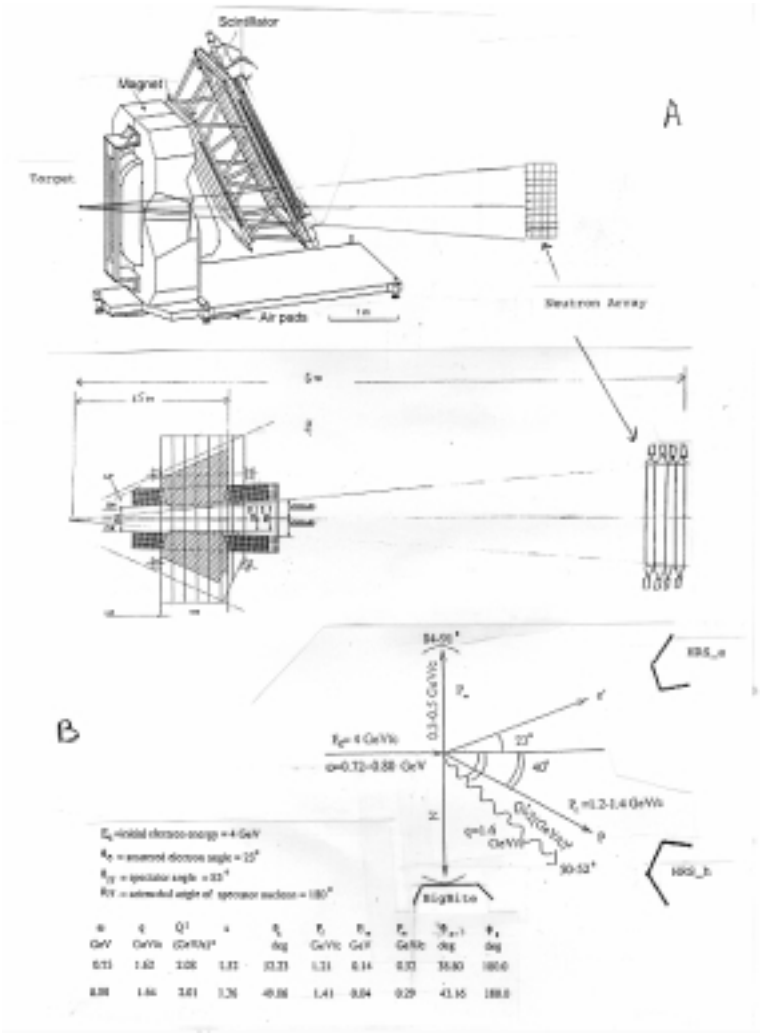

Figure 11: Proposed experimental setup for the $(e, e'p + \mathrm{N})$ triple coincidence measurements. Fig. 11A shows the BigBite and the neutron counters setup. Fig. 11B show kinematics and experimental setup of the HRS_e, HRS_h and Bigbite spectrometers to measure the reaction $(e, e'p + \mathrm{N})$ in "almost parallel geometry".

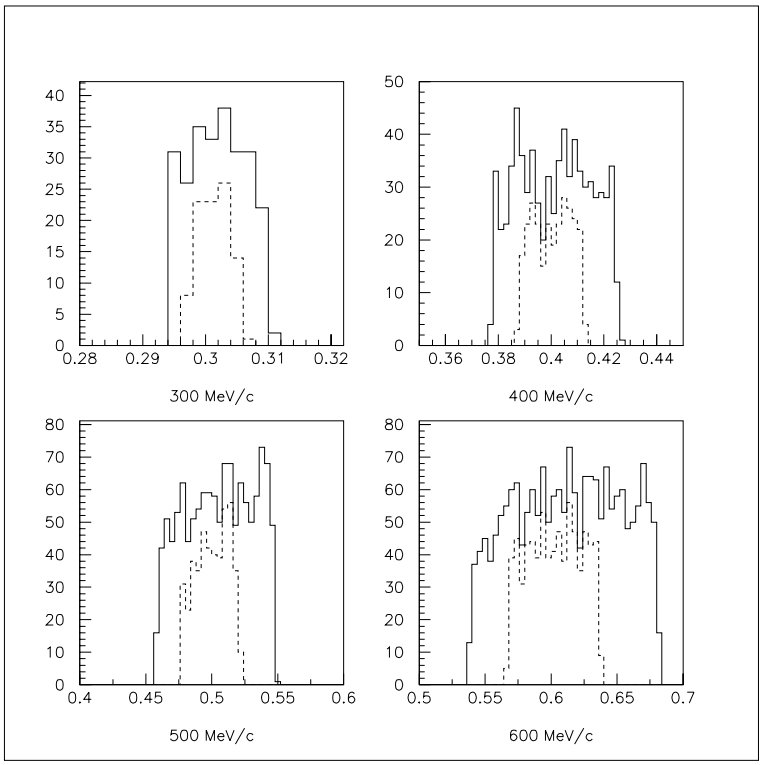

Figure 12: GEANT simulation of the measured momentum by BigBite using scintillators only. The solid line corresponds to a distance of 96.38 cm between the scintillator planes. The dashed line is for double this distance. The calculations are for point-like targets and for monochromatic protons of 300, 400, 500, and 600 MeV/c emerging from the target center.

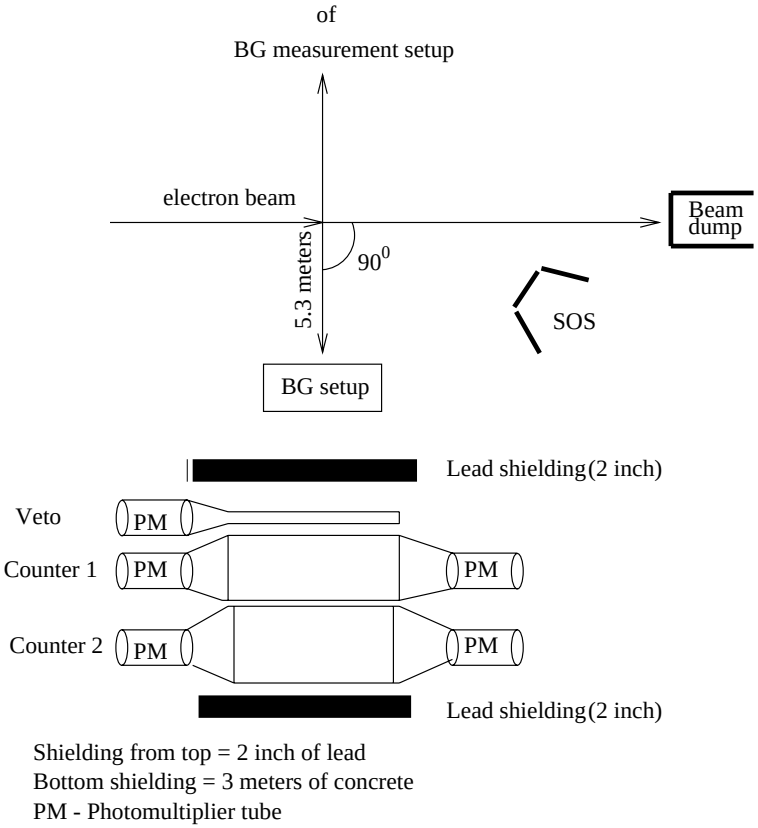

Figure 13: A schematic view of the set up used to measure the background in hall C.

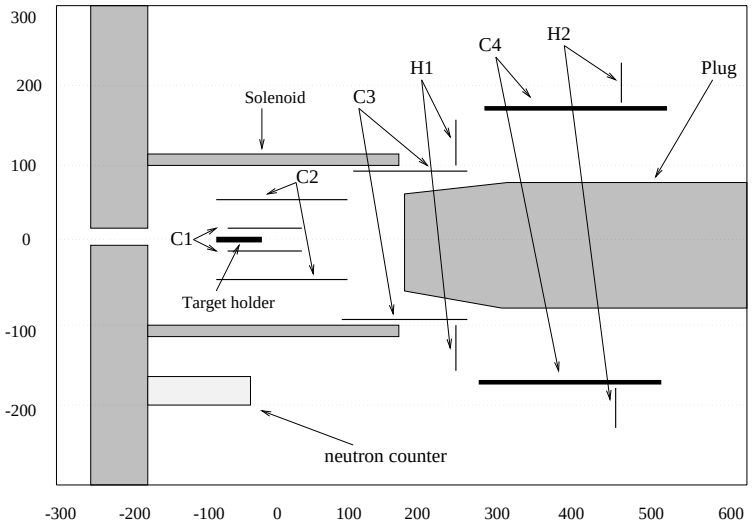

Figure I.1: Cross section of the EVA detector at BNL. The detector has cylindrical symmetry around the beam axis. The magnetic field lines emerging from the downstream end of the solenoid are collected and returned through the large iron plug. The scale in the figure is in centimeters. The C's are cylindrical drift chambers and the H's are scintillator hodoscopoes.

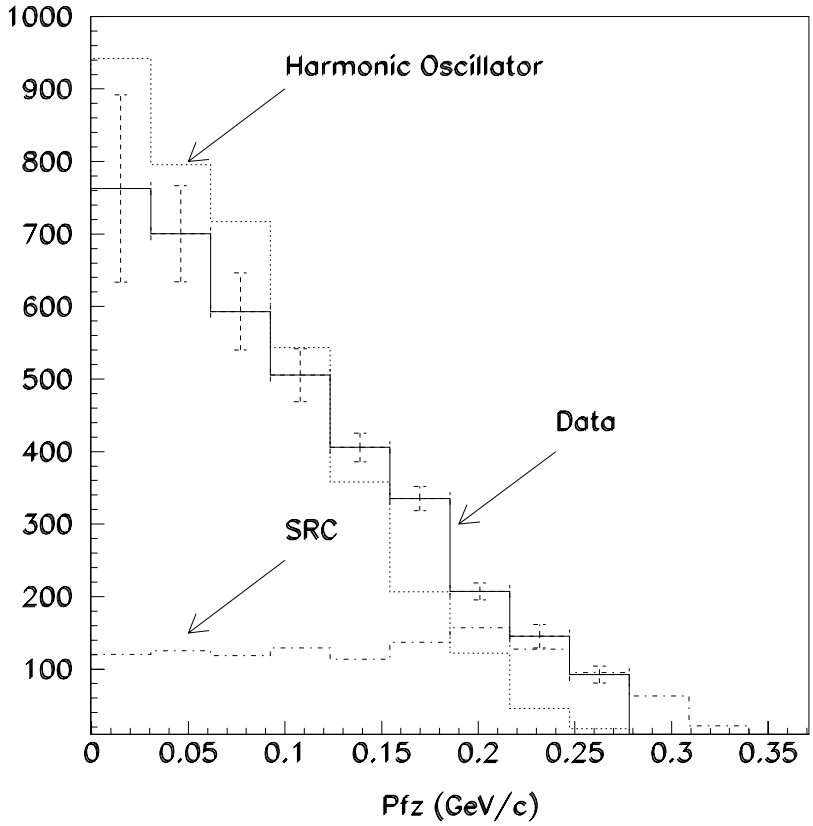

Figure I.2: P_{fz} is the longitudinal momentum distribution, obtained from the α distributions measured at 6 and 7.5 GeV/c and corrected for the s dependence induced by the elementary free cross section. HO is a harmonic oscillator independent particle model calculation. The P_{fz} and HO distributions are normalized to 1000 at the first bin. A model dependent SRC distribution is shown, arbitrarily normalized, just to show the shape.

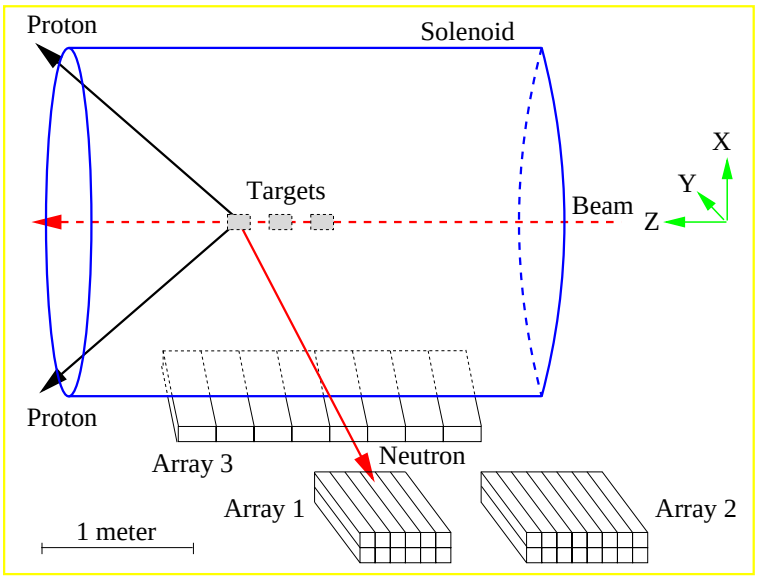

Figure I.3: A schematic view of the EVA solenoid and the neutron counters in the 1998 measurement.

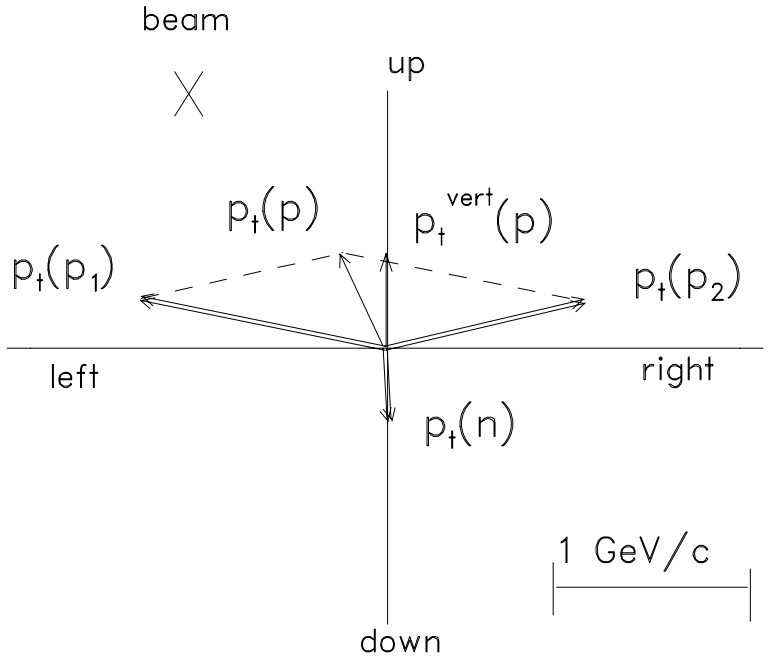

Figure I.4: A triple coincidence event measured at an incident momentum of 5.9 GeV/c. The vectors are projections on the plane normal to the incident beam. The axes are the vertical and horizontal directions in that plane. The $\mathbf{p}_t(p_1), \mathbf{p}_t(p_2)$ are the transverse momenta of the outgoing protons, $\mathbf{p}_t(p)$ is the transverse momentum of the target proton before the interaction and $p_t^{vert}(p)$ is its vertical component. $\mathbf{p}_t(n)$ is the projection of the neutron momentum on the same plane. The circle indicates the scale for a momentum of 220 MeV/c.

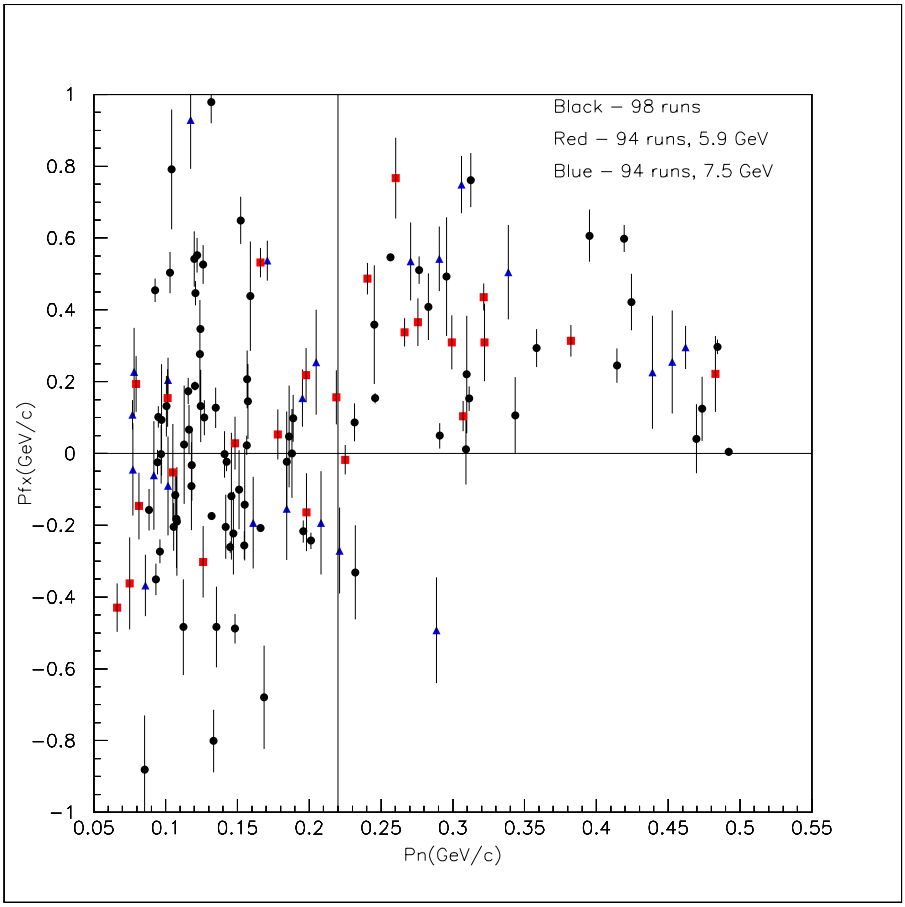

Figure I.5: The vertical component of the target nucleon momentum vs. the total neutron momentum.The positive vertical axis is the upward direction. The events shown are for triple coincidences of the neutron with the two high energy protons emerging from the QE C$(p, 2p)$ reaction. The squares are for the 5.9 GeV/c incident beam and the triangles are for 7.5 GeV/c. The dots are preliminary unpublished data from the 1998 runing period. We associate the events in the upper right corner with NN SRC.

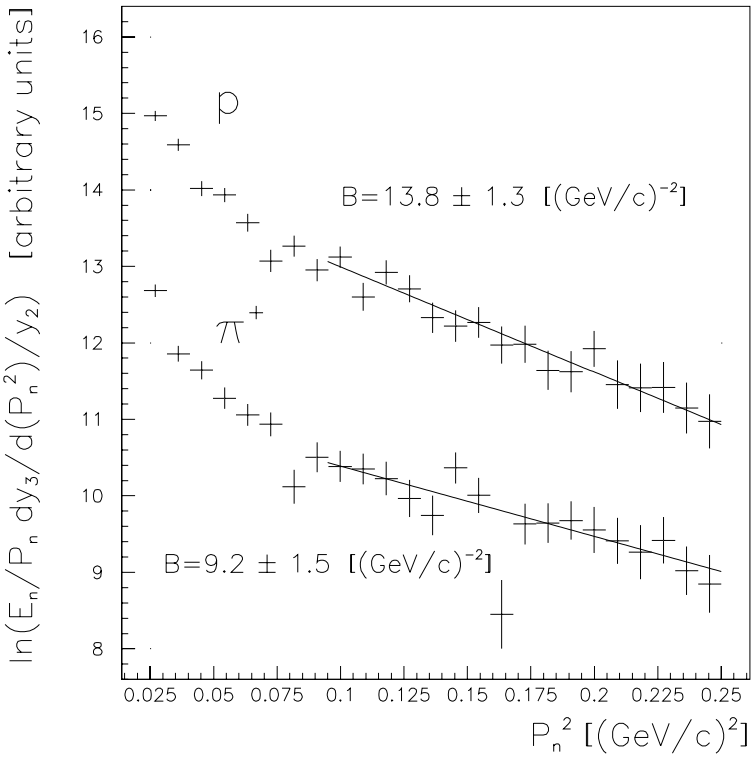

Figure I.6: Proton and pion induced neutron invariant momentum spectra. The vertical axis is $ln[(E_n/p_n) \times \frac{Y_3}{d(p_n^2)}]$, the horizontal axis is ${p_n}^2$. E_n and p_n are the energy and momentum of the neutron. Y_2 is the number of events with exactly two charged particles, each with $p_t > 0.6\mathrm{GeV}/c$, detected in the spectrometer. Y_3 is the effective number of Y_2 events that also have a single neutron entering the neutron counters. The neutron yield is corrected for the detection efficiency and attenuation. Above ${p_n}^2 > 0.1(\mathrm{GeV}/c)^2$ the points are fitted to a straight line. The B's are the slope parameters of the fitted straight lines.

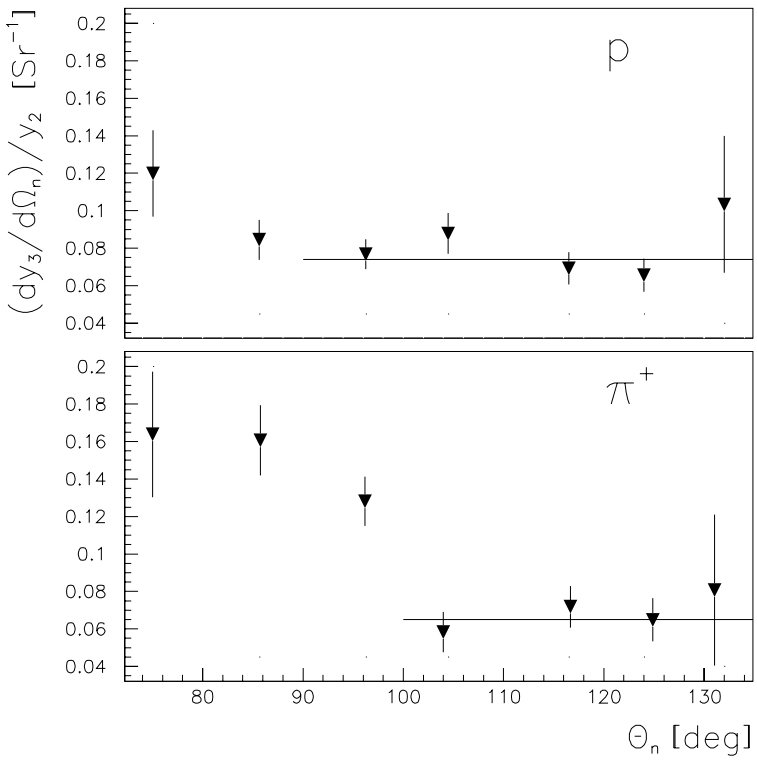

Figure I.7: The relative yield per solid angle $\frac{dY_3}{Y_2 d\Omega_n}$ of backward going neutrons above 0.32 GeV/c as a function of the neutron angle. Y_3 and Y_2 are defined in Fig. I.6 and the text. The data are for the proton and pion induced reactions. The lines represent fits to a constant which is used to estimate the total backward emission yield.

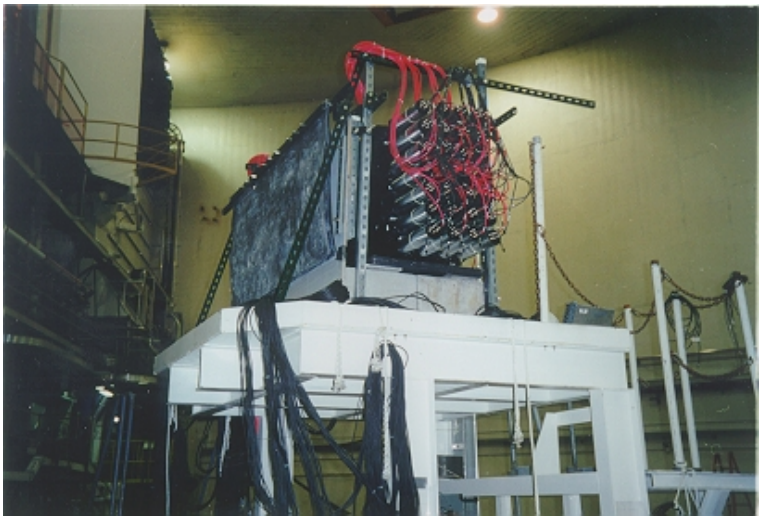

Figure II.1: Photo of the third arm in Hall A set for a parasitic measurement of the ^{3}He$(e, e'p + \mathrm{N})$ reaction during Feb 2000.

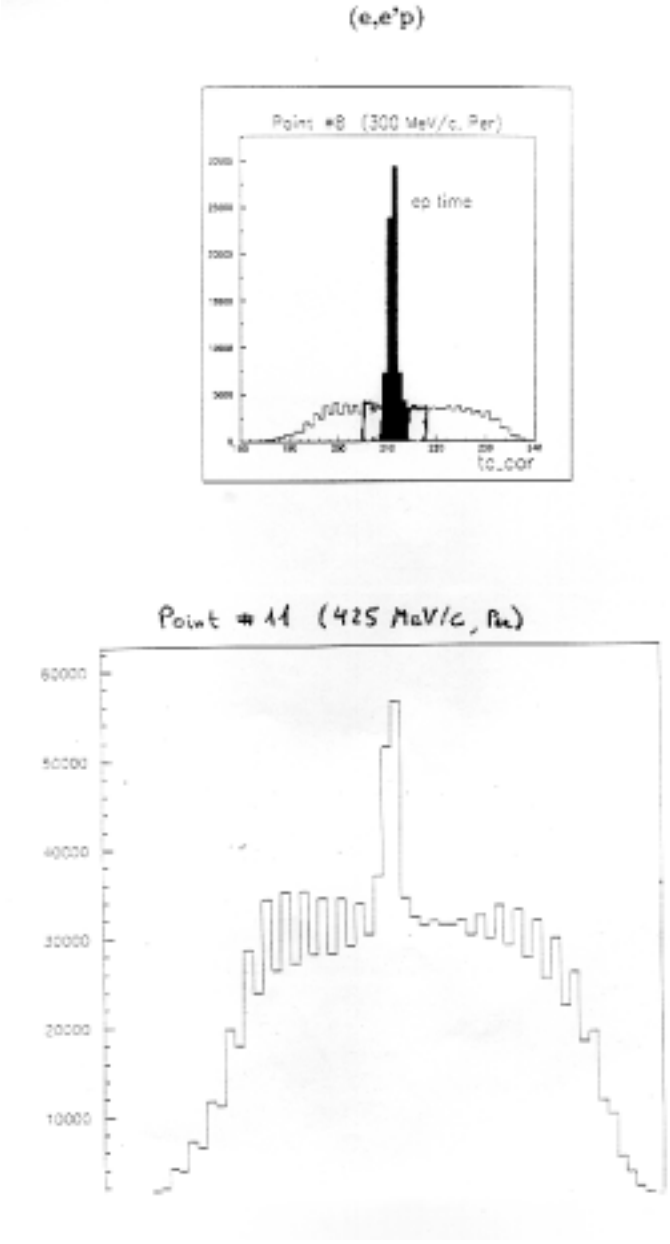

Figure II.2: The e-p time distribution for point 8 (low random coincidence rate) and point 11 (high random coincidence rate)

(e,e'p)

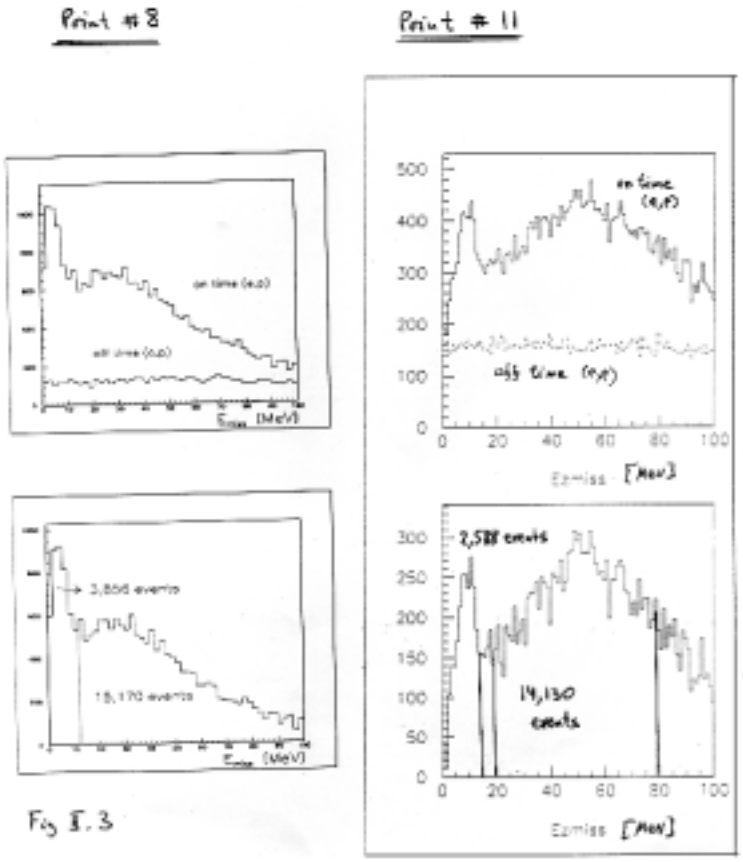

Figure II.3: The missing energy of the $(e, e'p)$ events. The full line correspond to a window on the e-p real coincidence time. The dashed lines are for a e-p time window equal in size to the real coincidence window but set at time correspond to random coincidences.

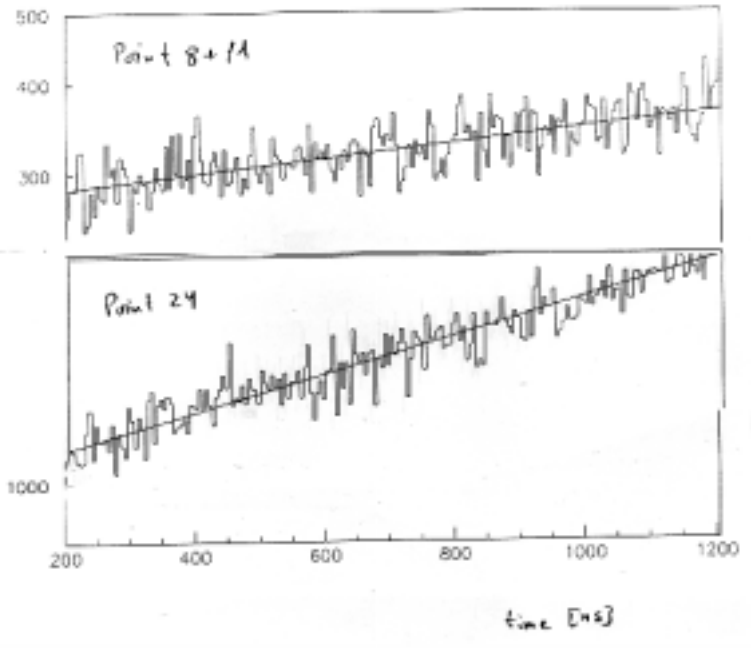

Figure II.4: Typical Time distributions for the neutrons in the array. The distributions are dominated by randoms and have exponential shapes.

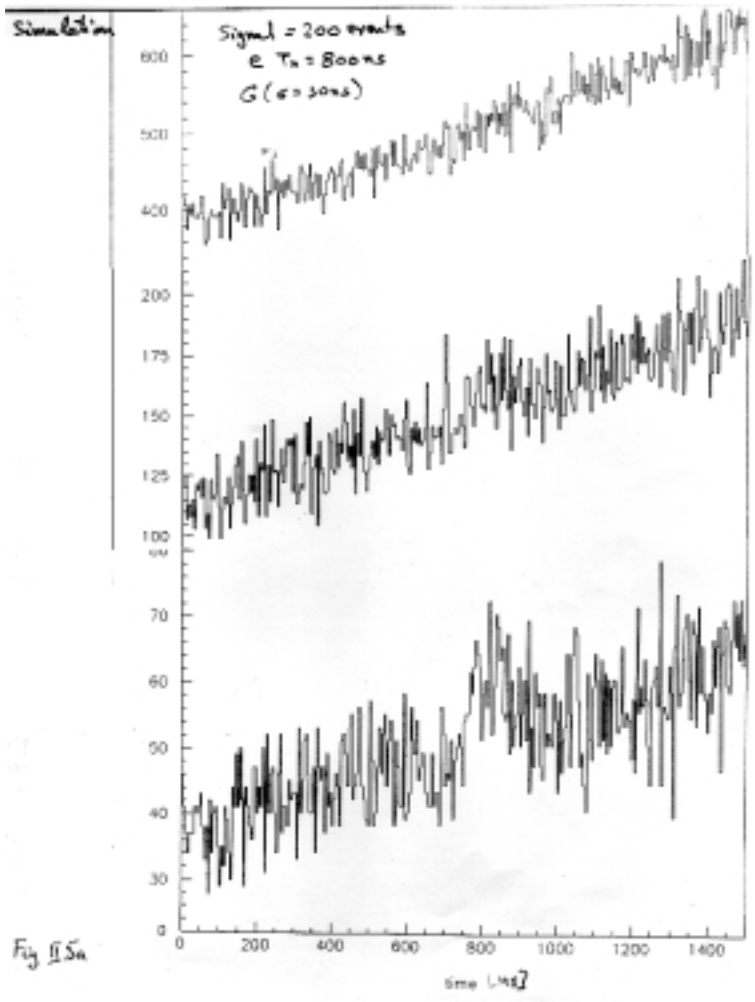

Figure II.5a: Simulation of a signal of 200 events on different random background levels. The signal is a Gaussian with width of 30 nsec and location at channel 800.

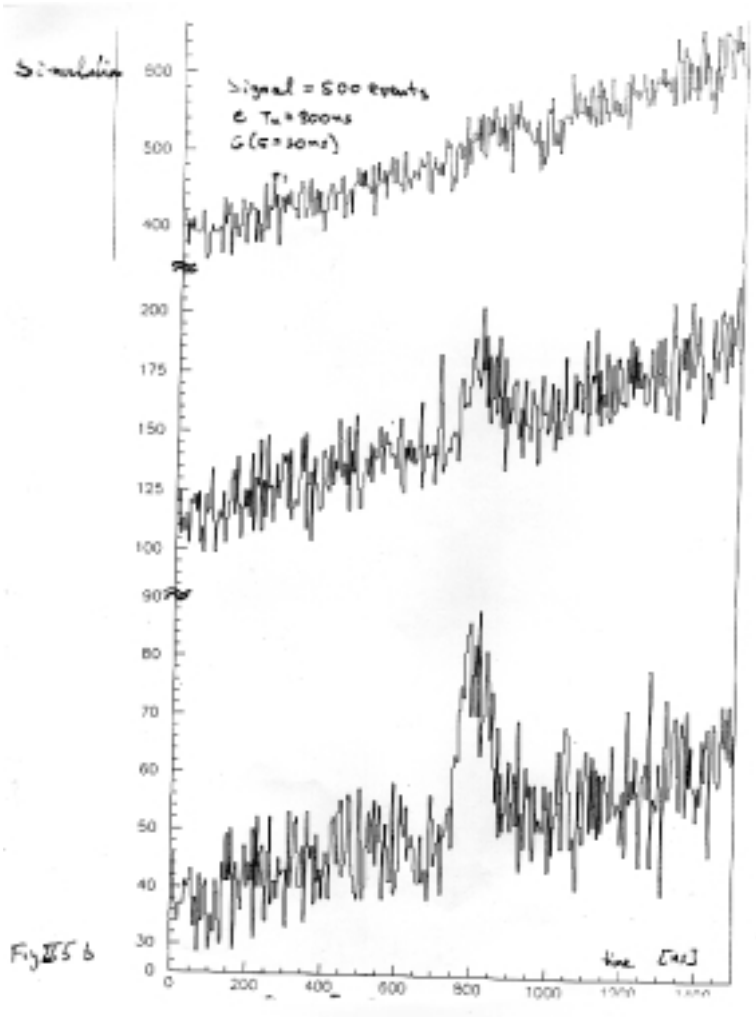

Figure II.5b: Same as figure II.5 but for 500 events.

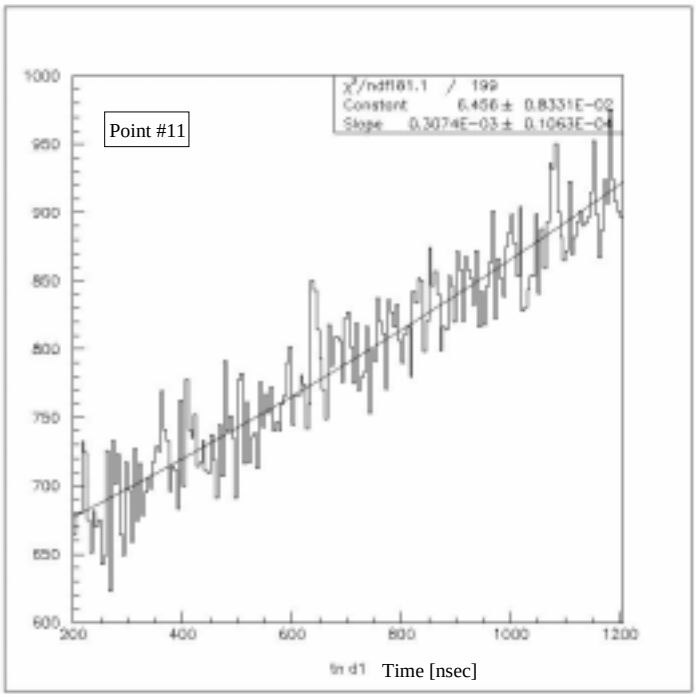

Figure II.6: The measured time distribution for point 11. These neutrons are in coincidence with $(e, e'p)$ events that passed the software cuts and that correspond to missing energy between 10 and 80 MeV. The upper limit on the $(e, ep+n)/(e, ep)$ ratio is set due to the fact that excess of 500 neutrons on top of the random background is clearly not consistent with the shown distribution.